

FOR REFERENCE

NOT TO BE TAKEN FROM THIS ROOM

METAL FLOW
IN
FORWARD COLD EXTRUSION

by

Raci ÖNELGE

B.S. in M.E., Bursa University, 1981

Submitted to the Institute for Graduate Studies in
Science and Engineering in partial fulfillment of
the requirements for the degree of

Master of Science

in

Mechanical Engineering

Bogazici University Library



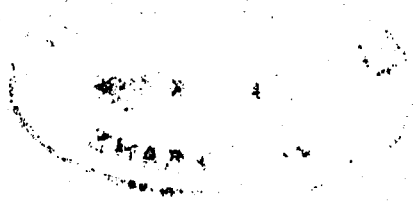
39001100314205

14

Boğaziçi University

1986

METAL FLOW
IN
FORWARD COLD EXTRUSION



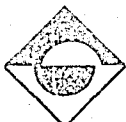
APPROVED BY

Doç.Dr.Sabri ALTINTAŞ *S. Altıntaş*
(Thesis Supervisor)

Doç.Dr.Öktem VARDAR ~~*Öktem Vardar*~~

Doç.Dr.Gülây AŞKAR *Aşkar*

DATE OF APPROVAL :



ACKNOWLEDGEMENTS

I would like to express my gratitude and sincere thanks to Doç.Dr. Sabri ALTINTAŞ, thesis supervisor, for his kind interest and guidance in the production of this work.

My special thanks are due to İhsan ÇAKIR, technical director in Kale Kalıp Fabrikası - Sefaköy / İstanbul, for his assistance.

Raci ÖNELGE

METAL FLOW
IN
FORWARD COLD EXTRUSION

ABSTRACT

In this work, experiments with a small-scale extrusion apparatus are described. Billets of commercially pure lead, which has the diameter of 50 mm were extruded at room temperature into 25 mm diameter solid bars at an extrusion rate of 2.5 mm/sec. Metal flow directions were determined during a small stepwise deformation process from distorted, originally square, grid-line network scribed on a meridian plane. Certainly, general agreement is found in the variation of the plastic region with die aperture and with mode of lubrication employed. It was further found that the metal located in the corner, formed by cylinder wall and die face, was in a state of plastic deformation. This observation shows that the surface quality of the finished extrusion is dependent on the surface quality of the billet from which the extrusion was pressed.

DOĞRUDAN SOĞUK EKSTRÜZYONDA METAL AKIŞI

ÖZET

Bu çalışmada, küçük bir ekstrüzyon düzeneğinde yapılan deneyler anlatılmaktadır. Bu deneylerde; çapı 50 mm olan ticari saflıktaki kurşundan yapılmış içi dolu takozlar, 2.5 mm/san'lik bir ekstrüzyon hızıyla, çapı 25 mm olan çubuklara ekstrüzyon edilmektedir. Metal akış yönleri meridyen düzlemine yapılan ızgaranın deformasyonu yoluyla tayin edilmektedir. Plastik bölgenin, kalıp şekli ve uygulanan yağ ile değişimi üzerine var olan genel düşünce doğrulanmıştır. Buna ek olarak, silindirin çeperi ve kalıp yüzü tarafında oluşan köşedeki metal yığılmasının plastik deformasyon durumunda olduğu bulunmuştur. Bu gözlemler; ekstrüzyon edilen çubuğun yüzey kalitesinin; ekstrüzyon edilecek takozun yüzey kalitesine yakından bağlı olduğunu göstermiştir.

TABLE OF CONTENTS

	Page
ACKNOWLEDGEMENTS.....	ii
ABSTRACT.....	iii
ÖZET.....	iv
LIST OF FIGURES.....	vii
LIST OF TABLES.....	ix
LIST OF SYMBOLS.....	x
I. INTRODUCTION.....	1
II. LITERATURE SURVEY.....	6
III. PHASES DURING EXTRUSION.....	8
A. Coining Phase.....	8
B. Steady State Phase.....	8
C. Unsteady State Phase.....	10
IV. THE THEORY OF EXTRUSION.....	11
A. Mathematical Formulation of a Problem of Plastic Flow.....	13
B. General Methods of Calculation.....	16
C. The Theoretical Extrusion Pressure.....	19
V. FLOW BEHAVIOUR DURING EXTRUSION.....	22
VI. DESIGN APPROACH TO FORWARD COLD EXTRUSION...	25
A. Calculation of the Work of Deformation and the Extrusion Load.....	25
1. Elementary Analysis.....	25
B. Design of Containers with Round Bores....	28
1. Design of Monobloc Containers.....	30
C. Stems for Rod Extrusion.....	32
D. Dies for Forward Cold Extrusion.....	33
VII. EXPERIMENTAL TECHNIQUE AND RESULTS.....	36
A. Extrusion Equipment and Billet Preparation	36
1. Extrusion Apparatus.....	38
a. Dies.....	38
b. Container.....	38
B. Heat Treatment and Lubrication.....	41
C. Description of Extrusion Tests and Results.....	41

	Page
VIII. METAL FLOW DURING EXTRUSION.....	46
APPENDIX.....	55
BIBLIOGRAPHY.....	61

LIST OF FIGURES

		<u>Page</u>
FIGURE 1	Schematic Diagram of Forward Extrusion Processes	3
FIGURE 2	Diagrammatic View of Indirect Extrusion Processes	4
FIGURE 3	Idealised Autographic Force-Punch Displacement Diagram for Forward and Backward Extrusion Illustrating the Phases of the Processes	9
FIGURE 4	Locations of Various Problem Areas Encountered in Deformation Processing Operations	12
FIGURE 5	Structure of an Ideal Extrusion Theory	17
FIGURE 6	Shape Changing Work Balance in Extrusion	17
FIGURE 7	Development of the Usual Logarithmic Extrusion Pressure Formula	19
FIGURE 8	Schematic Representation of Three Different Types of Flow Behaviour During Extrusion	22
FIGURE 9	The Major Features of a Cold Extrusion Die	34
FIGURE 10	The Geometric Variables in Forward Cold Extrusion	35
FIGURE 11	Extrusion Apparatus	37
FIGURE 12	Experimental Arrangements	37
FIGURE 13	Dies for Cold Extrusion of Solid Round Bars	39
FIGURE 14	Stress-Strain Curves for Lead in Compression	39
FIGURE 15	Casting Mold and Billet	40
FIGURE 16	Sectioned Billet	40

FIGURE 17	Cut Split Billet	41
FIGURE 18	Commercial Lead Alloy Split Bar Extruded with a 75 Per Cent Reduction through 60-Deg Die	43
FIGURE 19	Commercial Lead Alloy Split Bar Extruded with a 75 Per Cent Reduction through 150-Deg Die	44
FIGURE 20	Commercial Lead Alloy Split Bar Extruded with a 75 Per Cent Reduction through 180 (Flat)- Deg Die	45
FIGURE 21	Deformation Pattern, during Direct Extrusion of Square Grid Network on Meridian Plane of Lead Billet	47
FIGURE 22	Deformation Pattern, during Direct Extrusion of Square Grid Network on Meridian Plane of Lead Billet	48
FIGURE 23	Deformation Pattern, during Direct Extrusion of Square Grid Network on Meridian Plane of Lead Billet	49
FIGURE 24	Experimentally Observed Flow Pattern in Commercial Lead Alloy Extruded at Room Temperature and Ram Speed of 2.5 mm/sec.	50
FIGURE 25	Deformation Pattern, During Direct Extrusion of Square Grid Network on Meridian Plane of Lead Billet	51
FIGURE 26	Deformed Grid Network of Commercial Lead Alloy after Extrusion	52

LIST OF TABLES

	<u>Page</u>
TABLE 1 The theoretical extrusion pressure	21

LIST OF SYMBOLS

A	Corresponding cross-sectional area
A_0	Area of container bore
A_1	Initial cross section
A_2	Final cross section
b	Extrusion constant
d_1	Initial bar diameter
d_2	Final bar diameter
d_i	Inside diameter of monobloc container
d_a	Outside diameter of monobloc container
F_{id}	Ideal extrusion load
F_s	Stem load
F_a	Total load
F	Tensile load
l	The die land length
L_1	Length of bar before extrusion
L_2	Length of bar after extrusion
P_l	Logarithmic extrusion pressure
P_0	Minimum theoretical extrusion pressure
P	Maximum theoretical extrusion pressure
P_{ri}	Internal radial pressure
P_{ra}	External radial pressure
R	Extrusion ratio
$\frac{r}{R}$	Percentage reduction
$\frac{r}{R}$	Die entry radius
S	Safety factor
u	Diameter ratio
$\bar{u}, \bar{v}, \bar{w}$	Displacement components
v	Ram speed
V	Volume of the bar
W_a	Total work
W_f	Frictional work
W_h	The pure deformation work

W_i	The redundant or internal deformation work
Y	Yield strength
Y_w	Deformation resistance
α	The half angle
$\dot{\gamma}_{xy}, \dot{\gamma}_{yz}, \dot{\gamma}_{xz}$	Shear strain-rates
$\dot{\epsilon}_{xx}, \dot{\epsilon}_{yy}, \dot{\epsilon}_{zz}$	Direct strain-rates
ϵ	Strain
η	Deformation efficiency
λ	Non-negative parameter
μ	Coefficient of friction
μ_{cb}	Coefficient of friction between container and billet
μ_{db}	Coefficient of friction between die and billet
σ_{ij}	Stress tensor
$\bar{\sigma}$	Mean flow stress
σ'_{ij}	Deviator stress tensor
σ_m	Mean stress
σ_r	Radial stress
σ_θ	Tangential stress
σ_R	Resultant stress
\emptyset	The included die angle

Subscripts

r	Radial
θ	Tangential
z	The axis of symmetry
i, j, k	Indices
x	In x direction
y	In y direction
1	Initial
2	Final

I. INTRODUCTION

Cold extrusion of metals, particularly non-ferrous alloys has become a well-established and important manufacturing process. The principal application of the process was formerly in the production of ordinance items, such as mortar and artillery shells and cartridge cases. More recently, however, the process has gained considerable attention from the automative industry for the production of small parts, such as wrist pins, hydraulic valve plungers and electrical switch housings. It has inherent advantages to other processes such as rolling, and forging in that complicated shapes with re-entrant angles can be obtained readily with this process and that the dies are relatively simple, easily manufactured, and replaced in an extrusion press, if it is desired to alter the shape of the product.

Some of the advantages that are gained by cold extrusion are (1):

1. Conversion of low-strength alloys to high-strength finished products through work-hardening.
2. Saving of time and material because of fewer operations and smaller machining losses.
3. Production of an uninterrupted fiber flow, which results in greater load carrying capacity.

4. Good surface finish and maintenance of tolerances within close limits.

The process consists of placing a roughly fitting cylindrical billet in the cylinder of an extrusion press and forcing the metal through a steel or carbide aperture having the desired shape of the product; it is somewhat analogous to forcing tooth paste out of the orifice of a tooth-paste tube.

Two methods of applying the extrusion pressure are commonly used and are illustrated schematically in Fig. 1 and 2 (2,3).

a. Direct Extrusion Process The pressure is applied by means of the hydraulically operated ram at one end of the billet through a follower plate or piston (Fig. 1)

The forming pressure is transmitted through the billet in forcing the metal through the die at the other end of the billet.

b. Indirect or Inverted Extrusion Process The pressure is applied though the die itself fixed to the hydraulically operated ram and extruded product enters the hollow ram. (Fig. 2)

The direct extrusion process has the advantage that the length of the product is limited only by the size of the billet or the length of the runout table (4). Its disadvantage lies in the fact that the forming pressure, in addition to causing plastic flow in the metal, must be sufficiently high to overcome friction induced at the wall of the cylinder, since the billet moves relative to the cylinder. In the inverted or indirect extrusion

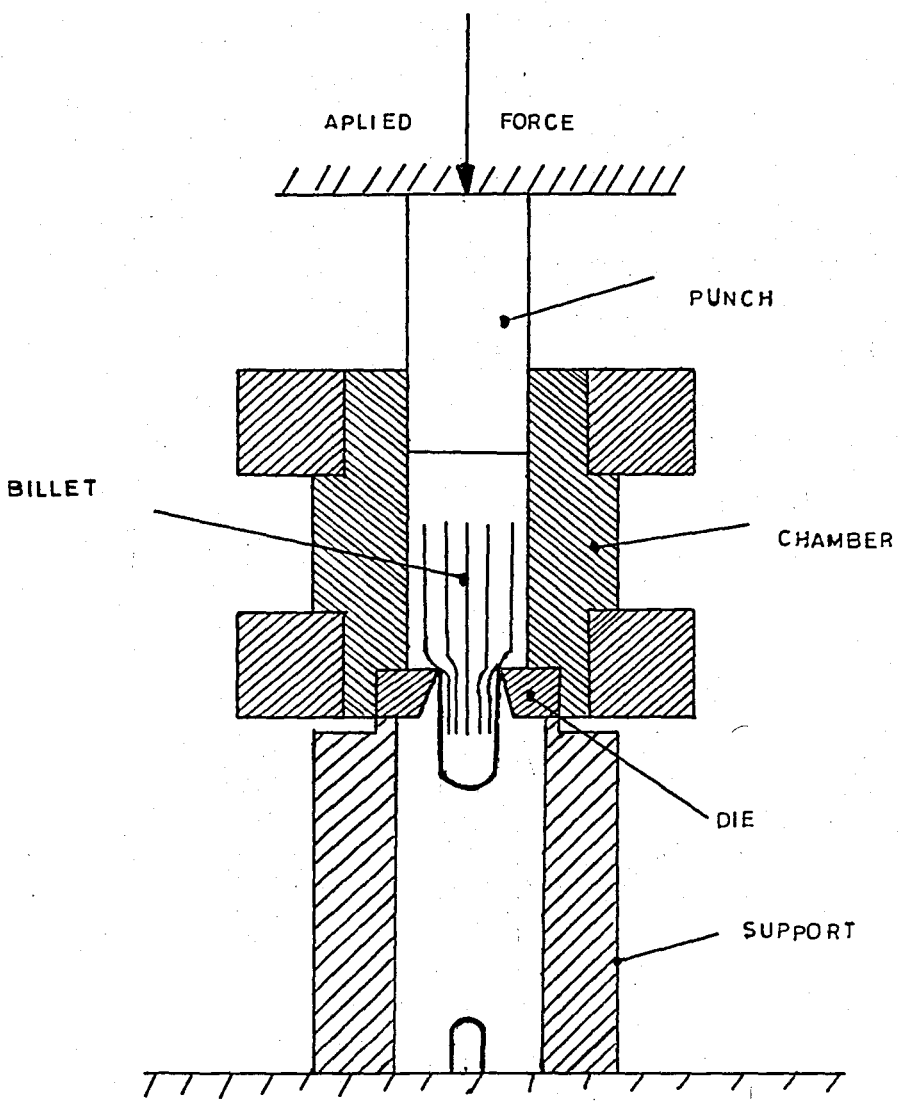


FIGURE 1- Schematic Diagram of Forward Extrusion Processes (2)

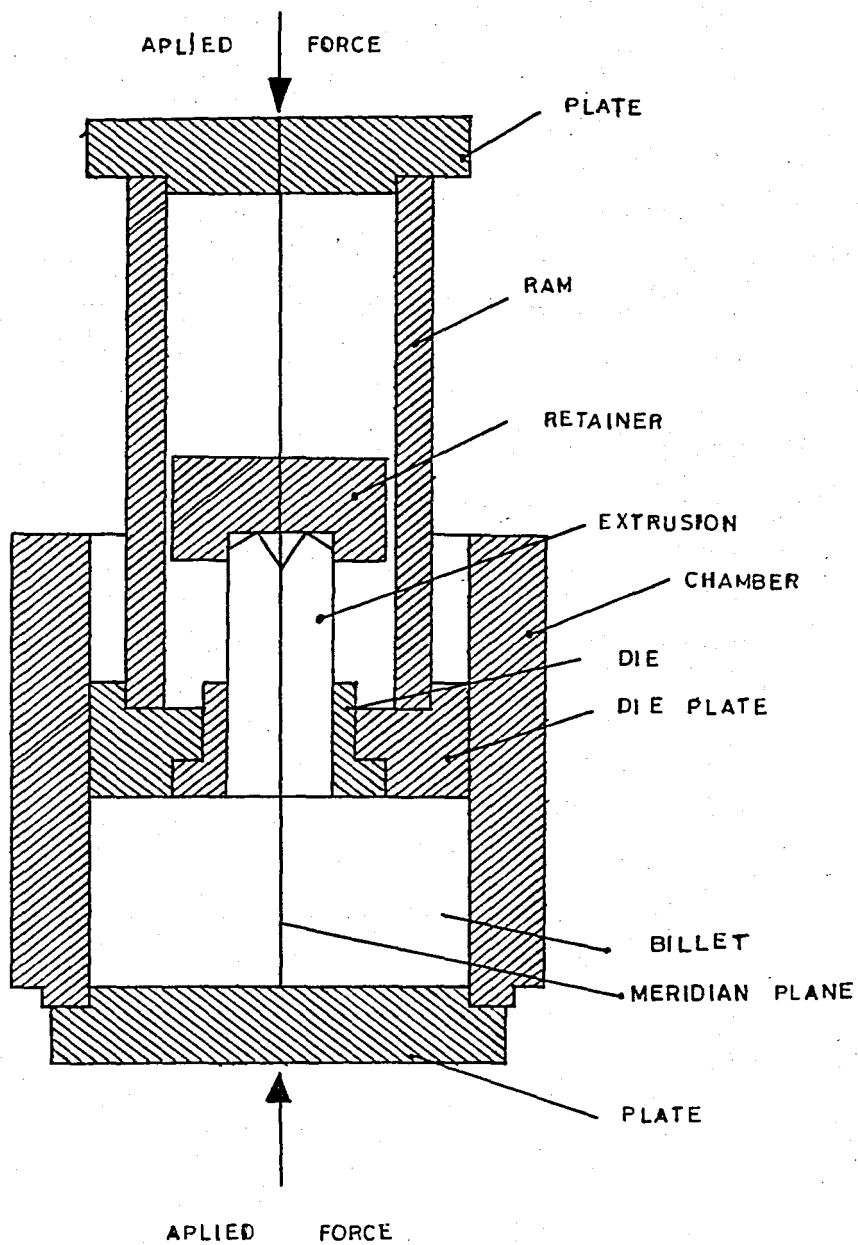


FIGURE 2- Diagrammatic View of Indirect Extrusion Processes (3)

Process the cylinder-wall friction is reduced materially, since little relative motion exists between billet and cylinder wall, but the length of the extruded product is limited by the length of the hollow ram.

The factors of the deforming mechanism in extrusion are extrusion pressure, rate, temperature, reduction, the shape of die and lubricants. Generally, the relation between metal flow and the shape of die and lubricants is considered to be important (5)

The aim of this study is to search for the relation between metal flow and die shape by experiments. The way of extrusion is forward extrusion of lead split billet at room temperature. A study of flow patterns is of great importance in extrusion since it is an aid in the proper design of dies and in the determination of process variables.

II. LITERATURE SURVEY

Extrusion is one of the youngest of the metal forming processes. Pearson and Parkins (6) have pointed out that the principle of extrusion was apparently first applied by J. Bramah of Sheffield who, in 1797, invented a machine to extrude lead pipes.

Experiments with a laboratory extrusion apparatus under conditions of plane strain were made in 1953 by Purchase and Tupper (7). In the same year, Plastic flow in a lead extrusion was studied by Yang and Thomsen (8) In 1954, an experimental study of metal extrusions at various strain rates was undertaken by Frisch and Thomsen (3) 1955 to 1956, stresses and strains in cold-extruding 2S-0 aluminium, experimental and theoretical pressures and velocity fields for various lead extrusions, and the effect of process variables on extrusion pressures of lead were considered by Thomsen and Frisch (8-10). Important contributions to the extrusion production of non-ferrous metals and alloys have been made by Avitzur (11-14), and his co-workers (15) carried out very original investigations into extrusion in order to establish the relationships between the extrusion force, the characteristic parameters of the process.

Later, an attempt was made to examine the potential theory in 1967 by Shabaik, Kobayashi, and Thomsen (2). It was found that by the proper adjustment of the boundary configuration for cases where the flow changed direction gradually, the agreement between theory and experiment was excellent. In 1968, Theoretical and experimental flow

fields of several extrusion ratios of lead extruded in plane strain were compared by Shabaik and Thomsen (16).

Later; Iwata, Osakada and Fujino (17) developed the analysis of hydrostatic extrusion by the finite element method; an elasto-plastic analysis of hydrostatic extrusion was made using the finite element method. After a technique of semi-empirical analysis, based on strain distribution measurements and known as the viscoplasticity method, had been developed by Thomsen, Frisch and other co-workers (3,9, and 10) which had made contributions to a better understanding of some complicated problem, viscoplasticity analysis of 2024 aluminium alloy extrusions was considered by Medrano, Hinesley, Gills and Conrad (18).

In 1981, the influence of temperature and ram speed in hot extrusion of aluminium alloys were considered by Sheppard (19).

III. PHASES DURING EXTRUSION

Typical extrusion force-punch displacement autographic diagram for the slow forward and backward cold extrusion of a cylindrical slug (billet) of a well-lubricated non-hardening material through a single circular orifice, square-faced die is shown in Figure 3. Examination of this diagram suggests that there are three principal phases during the processes which can be distinguished as (a) the coining phase, (b) the steady state phase and (c) the post-steady or unsteady state phase (20)

A. Coining Phase

At the commencement of an extrusion, the billet initially deforms elastically in compression, yields in the vicinity of the die and then in this region deforms plastically to exactly fill the die and the container which expand elastically. At the same time there is usually a limited amount of extrusion of relatively unstrained material. During this coining phase the extrusion force is therefore expected to increase rapidly.

B. Steady State Phase

As the extrusion proceeds and the punch continues to move forward in a forward or direct extrusion the extrusion force decreases. This occurs because the frictional resistance at the container interface decreases as the length of undeformed billet diminishes. However, during backward or indirect extrusion, there is no relative motion between the billet and the container and consequently

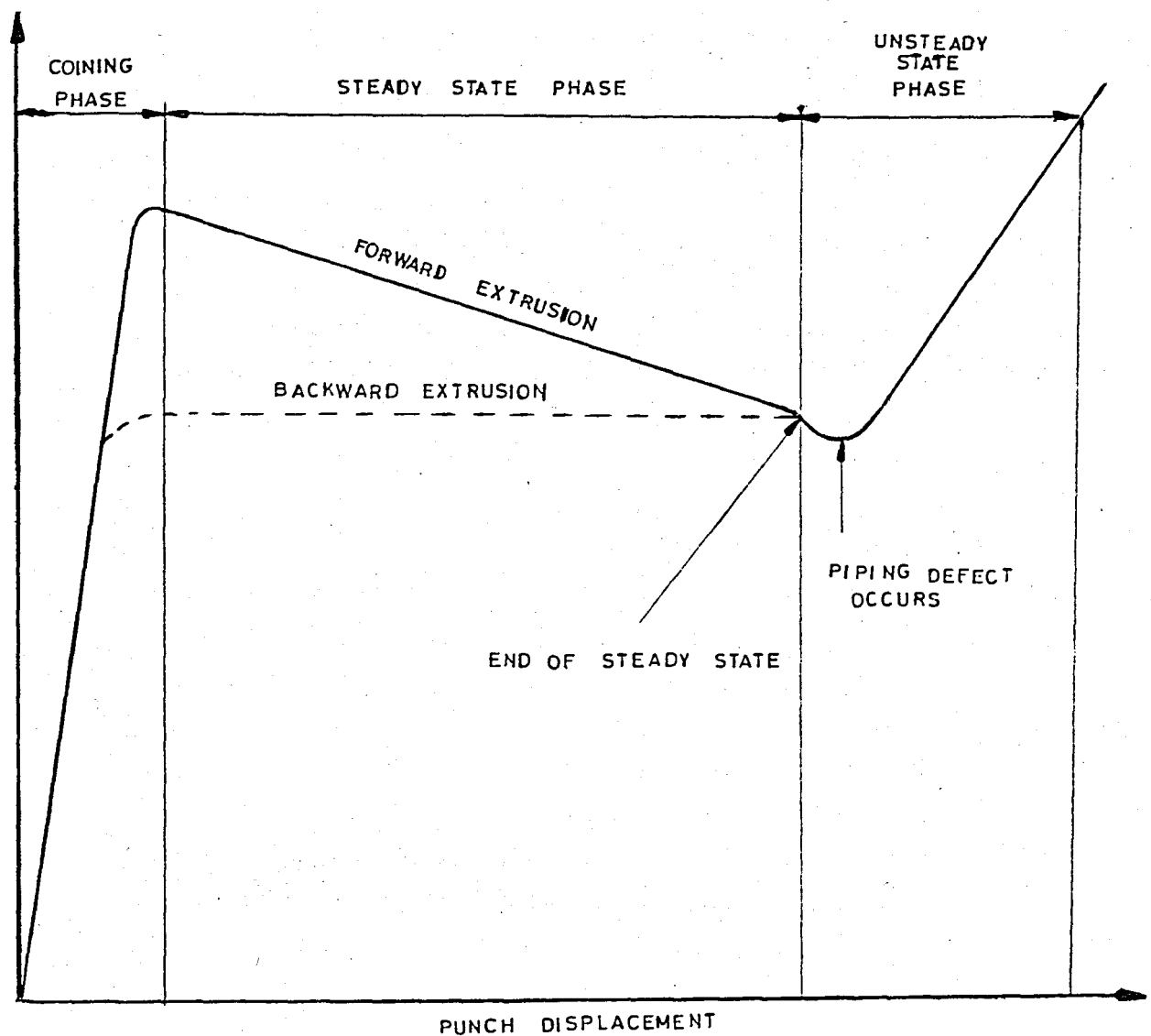


FIGURE 3- Idealised Autographic Extrusion Force-Punch Displacement Diagram for (a) Forward or Direct Extrusion, and (b) Backward or Indirect Extrusion Illustrating the Phases of the Processes (20)

frictional resistance is absent. The extrusion force therefore remains sensibly constant during this phase.

C. Post-Steady or Unsteady State Phase

A more rapid rate of decrease in the extrusion force is evident at the end of the steady state phase. The whole of the billet now constitutes the zone of plastic deformation and the field of strain changes as the punch advances. When the length of billet is reduced to about half the diameter of the extruded product, a cavity or so-called pipe is initiated on the axis at the rear end of the billet and the final phase of unsteady state deformation occurs.

The cavity gradually increases in diameter and depth so that the extruded product during this phase is transformed into a pipe of increasing internal diameter. This extrusion defect of piping occurs at some point in the process when the velocity of the billet at the axis of symmetry exceeds the velocity of the punch. The material in the vicinity of the axis breaks contact with the punch and the cavity begins to form. The extrusion force is no longer uniformly distributed over the whole of the pressure pad.

IV. THE THEORY OF EXTRUSION

Practical extrusion shares two important features with most other deformation-processing operations: it is extremely complex and its practice is far ahead of its theory. The latter is clearly a fortunate circumstance, considering the state of the theory.

Most of the operations that depend upon deformation for shape changing and property control also share a number of common problem areas. Their relative importance and degree of interaction may change with the operation, but they can usually be identified, if only in a broad way. Five problem areas are indicated in just this way for the example of extrusion in Figure 4. (21).

Area 1 represents the deformation zone, generally regarded as the province of continuum mechanics and applied mathematics. There is concern here over the distribution of stress, displacements, and strain, the overall pressure requirements and problems of die design as well;

Area 2 covers the interface between the elastically loaded tools, (tool, container, etc.) and the plastically deforming billet. There is strong interaction with other areas, especially 1. The concern is now with the difficult questions of heat transfer, friction, and lubrication under the unique conditions of plastic working, tool wear, and resulting surface;

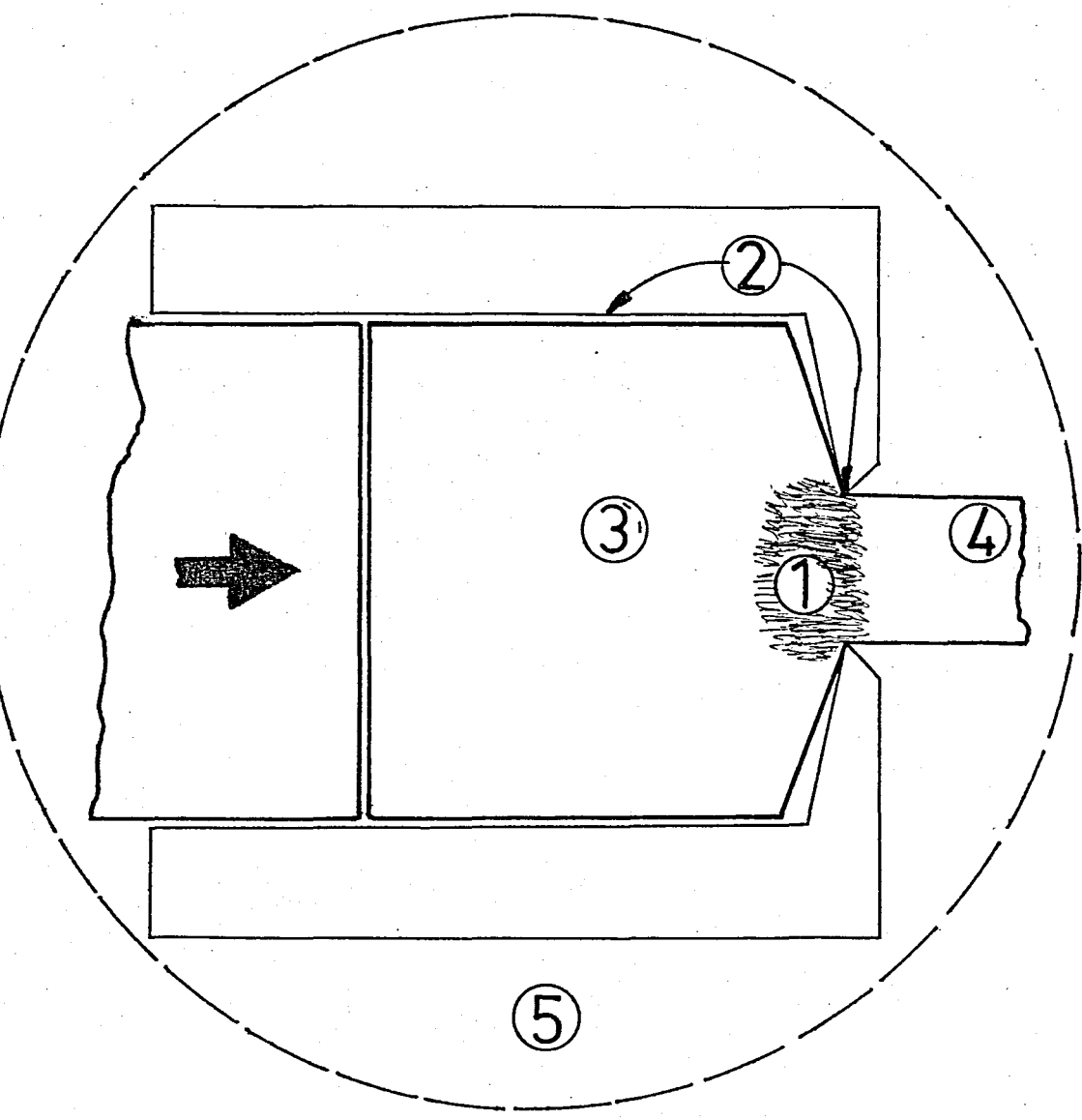


FIGURE 4- Locations of Various Problem Areas Encountered in Deformation Processing Operations (21)

Area 3 embraces the properties and characteristics of materials under conditions of processing. This is a critical, but rather neglected, metallurgical problem area, generally centered around strain hardening, recrystallization, fracture, etc. Very often the specific conditions of interest involve high temperatures and high strain rates, but these in turn may be only ill defined. Here is where the perennial problem of workability evaluation lies;

Area 4 is strongly metallurgical, based on structure and properties and how these are influenced by the deformation; and

Area 5 loosely represents the whole processing system and includes the primary deformation equipment plus auxiliary gear for heating, handling, etc. It clearly represents an area of much engineering activity.

In a simplified theoretical approach, therefore, the following variables can be considered as relevant (22)

- (a) Type of extrusion
- (b) Reduction
- (c) Die shape
- (d) Frictional conditions at the die and chamber wall.
- (e) Nature of the dead metal.

This leaves aside considerations of hardening, strain-rate effects, temperature effects, etc.

A. Mathematical Formulation of a Problem of Plastic Flow (21)

Mathematically, the problem of deformation of a rigid/plastic, non-hardening material may be couched in

the following terms. The complete state of stress at a point can be expressed in terms of six independent quantities which constitute the stress tensor. Relative to three mutually orthogonal axes x, y, z , these may be taken as $\sigma_{xx}, \sigma_{yy}, \sigma_{zz}, \tau_{yz}, \tau_{zx}, \tau_{xy}$, or collectively (and conventionally) by the array:

$$\sigma_{ij} = \begin{bmatrix} \sigma_{xx} & \tau_{xy} & \tau_{xz} \\ \tau_{xy} & \sigma_{yy} & \tau_{yz} \\ \tau_{xz} & \tau_{yz} & \sigma_{zz} \end{bmatrix}$$

In order that the resultant force acting on any element shall be zero (in the absence of body forces), these components must satisfy the following partial differential equations:

$$\frac{\partial \sigma_{xx}}{\partial x} + \frac{\partial \tau_{xy}}{\partial y} + \frac{\partial \tau_{xz}}{\partial z} = 0,$$

$$\frac{\partial \tau_{xy}}{\partial x} + \frac{\partial \sigma_{yy}}{\partial y} + \frac{\partial \tau_{yz}}{\partial z} = 0,$$

$$\frac{\partial \tau_{xz}}{\partial x} + \frac{\partial \tau_{yz}}{\partial y} + \frac{\partial \sigma_{zz}}{\partial z} = 0,$$

These are the stress-equilibrium equations and will be familiar to those who have a knowledge of elasticity. This expresses the stress components when the material deforms plastically. For convenience it will be said that plastic flow can occur when some (known) functional relation between the stresses is zero, i.e:

$$f(\sigma_{ij}) = 0.$$

In the non-deforming, or rigid regions, $f(\sigma_{ij}) \leq 0$. The displacement of any point during a small time interval, δt , is expressible in terms of three components, \bar{u}_x , \bar{v}_y , \bar{w}_z , in the x, y, and z directions, respectively. If these are related to the displacement of some convenient datum, e.g. the ram in extrusion, in the same time interval, they can be regarded as "velocities" \bar{u} , \bar{v} , and \bar{w} . It must be emphasized, however, that these velocities are not time rates. A set of strain rates in terms of these velocities can be formally defined, as in hydro-dynamics, by:

$$\dot{\epsilon}_{xx} = \frac{\partial \bar{u}}{\partial x} ; \quad \dot{\epsilon}_{yy} = \frac{\partial \bar{v}}{\partial y} ; \quad \dot{\epsilon}_{zz} = \frac{\partial \bar{w}}{\partial z}$$

$$\dot{\gamma}_{yz} = \frac{1}{2} \left(\frac{\partial \bar{w}}{\partial y} + \frac{\partial \bar{v}}{\partial z} \right); \quad \dot{\gamma}_{zx} = \frac{1}{2} \left(\frac{\partial \bar{u}}{\partial z} + \frac{\partial \bar{w}}{\partial x} \right)$$

$$\dot{\gamma}_{xy} = \frac{1}{2} \left(\frac{\partial \bar{v}}{\partial x} + \frac{\partial \bar{u}}{\partial y} \right);$$

The relations between the stress and strain rates corresponding to Hooke's law of elasticity, are the Lévy-Von Mises relations, namely:

$$\frac{\dot{\epsilon}_{xx}}{\sigma'_{xx}} = \frac{\dot{\epsilon}_{yy}}{\sigma'_{yy}} = \frac{\dot{\epsilon}_{zz}}{\sigma'_{zz}} = \frac{\dot{\gamma}_{yz}}{2\tau_{yz}} = \frac{\dot{\gamma}_{zx}}{2\tau_{zx}} = \frac{\dot{\gamma}_{xy}}{2\tau_{xy}} = \dot{\lambda}.$$

The components σ'_{xx} , σ'_{yy} , σ'_{zz} , are $\sigma_{xx} - \sigma_m$, $\sigma_{yy} - \sigma_m$, $\sigma_{zz} - \sigma_m$ where $3\sigma_m = \sigma_{xx} + \sigma_{yy} + \sigma_{zz}$; $\dot{\lambda}$ varies both with position and ram movement and is not a constant for the material. The equations given, together with the boundary conditions of the particular problem, govern the solution of a problem of plastic flow.

In cylindrical symmetry; the conditions are $\tau_{z\theta} = \tau_{r\theta} = 0$, $\bar{v} = 0$, and 4 stress and 2 velocity components are unknown in the cylindrical coordinate system (r, θ, z) with the z axis as the axis of symmetry,

$$\frac{\partial \sigma_r}{\partial r} + \frac{\partial \tau_{rz}}{\partial z} + \frac{\sigma_r - \sigma_\theta}{r} = 0,$$

$$\frac{\partial \tau_{rz}}{\partial r} + \frac{\partial \sigma_z}{\partial z} + \frac{\tau_{rz}}{r} = 0,$$

$$\frac{\dot{\epsilon}_r}{\sigma_z - \sigma_m} = \frac{\dot{\epsilon}_\theta}{\sigma_\theta - \sigma_m} = \frac{\dot{\epsilon}_z}{\sigma_z - \sigma_m} = \frac{\dot{\gamma}_{rz}}{2\tau_{rz}},$$

$$\frac{1}{2} \{ (\sigma_r - \sigma_\theta)^2 + (\sigma_\theta - \sigma_z)^2 + (\sigma_z - \sigma_r)^2 \} + 3\tau_{rz}^2 = \sigma_R^2$$

where $\sigma_R =$ Equivalent stress.

$$\text{and } \dot{\epsilon}_r = \frac{\partial \bar{u}}{\partial r}, \quad \dot{\epsilon}_\theta = \frac{\bar{u}}{r}, \quad \dot{\epsilon}_z = \frac{\partial \bar{w}}{\partial z}$$

$$\dot{\gamma}_{rz} = \frac{\partial \bar{u}}{\partial z} + \frac{\partial \bar{w}}{\partial r}.$$

B. General Methods of Calculation (21)

Starting with data like that at the left in Fig. 5 they lead to values for pressure requirements but not along a route through the "THEORY BOX". Their essential features can be illustrated with some discussion of a work balance that applies to all kinds of extrusion, and in principle, to any other plastic working operation as well. The terms, represented in Fig. 6, are the following:

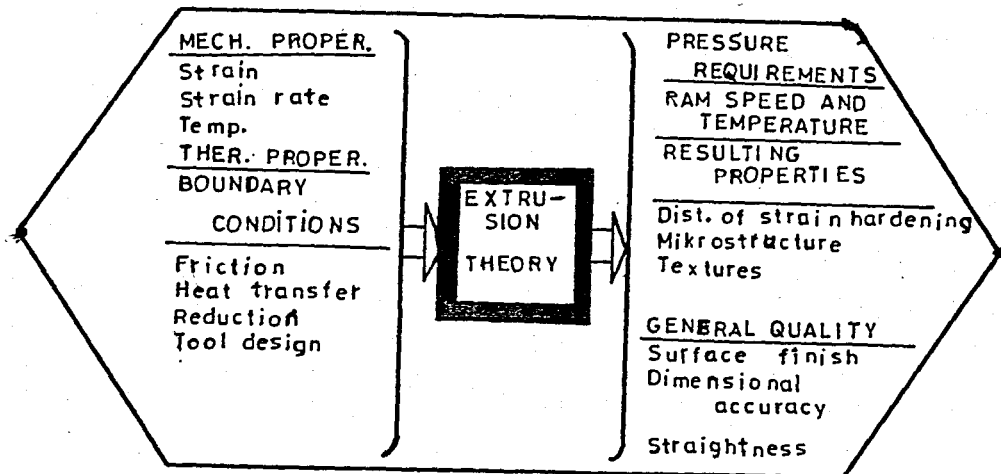


FIGURE 5- Structure of an Ideal Extrusion Theory (21).

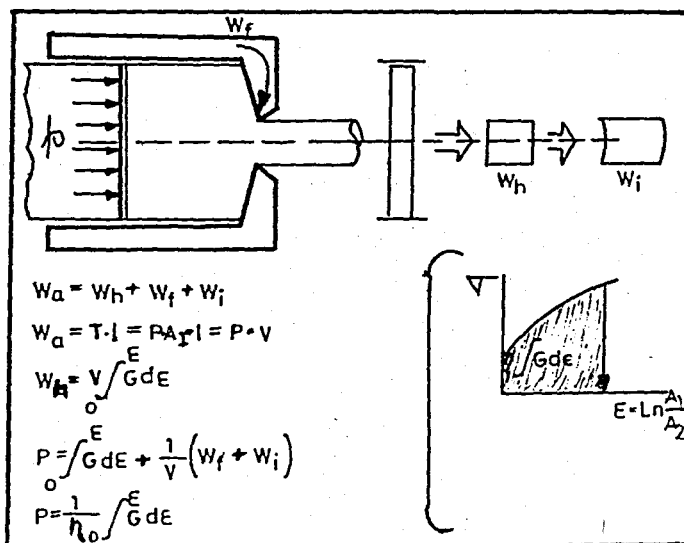


FIGURE 6- Shape Changing Work Balance in Extrusion (21).

W_a = total work actually required to extrude a billet of initial cross section, A_1 , and length, L , and volume $V = A_1 \cdot L$; this is the sum of:

W_h = the pure deformation work for homogeneous reduction of the volume from the initial to final cross section, indicated by the uniform compression of an initially thin, vertical and parallelsided element in the billet;

W_i = the redundant or internal deformation work expended in straining not required for the pure shape change, indicated by shear added to the uniformly-reduced element; and

W_f = work done in overcoming frictional resistance at container and die face.

Both W_a and W_h are directly evaluated as shown by the few equations. W_h per unit volume is simply the area under a true stress-strain curve for the material and conditions of extrusion, whatever they are, up to strain $\epsilon = \ln(A_1/A_2)$ set by the reduction from A_1 to A_2 , or extrusion ratio $A_1:A_2$. To produce the last equation a shape-changing or deformation efficiency, η , is introduced, which is nothing but the fraction of all work done solely for the necessary shape change. This step collects into one quantity the much less clearly resolved work losses, W_f and W_i .

The development of explicit expression for η , usually in terms of die profile, friction coefficient, and billet geometry, has, in effect, constituted much of the past work on calculation methods. Also needed for use of the last equation is the material's strain-hardening behaviour

under extrusion conditions. A usual, and often reasonable, assumption is illustrated in Figure 7; the integral quantity, $\int \sigma d\epsilon$, can be approximated by the product of a deformation strength, or mean flow stress, and the overall strain. Then the equation can be rewritten as shown with a quantity $b = \bar{\sigma}/\eta$, which is frequently termed the extrusion constant.

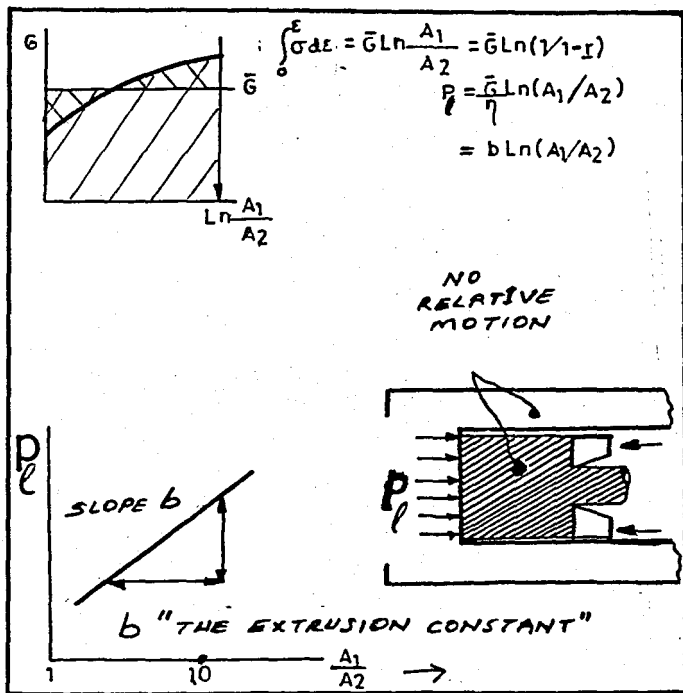


FIGURE 7- Development of the Usual Logarithmic Extrusion Pressure Formula (21).

C. The Theoretical Extrusion Pressure

Several methods for calculating the extrusion pressure have been developed since the start of systematic extrusion research. They differ from each other in the assumptions made, the method and complexity of analysis, the theoretical

basis and the degree of approximation of the solution (1). The study in Ref. (21) considers that the relation between the shape of the die and the extrusion pressure to be most important. The shape of the die means, half angle of the die. The minimum extrusion pressure is given as (21).

$$P_0 = Y \left\{ \frac{1+C}{C} \left(\frac{d_2^2}{d_1^2} \right)^C - 1 \right\} + \frac{2}{\sqrt{3}} Y \left(\frac{\pi}{\sin 2\alpha} - \cot \alpha \right)$$

$$\text{when } \alpha \neq \frac{\pi}{2}$$

$$P_0 = Y \ln \left(\frac{d_2^2}{d_1^2} \right) + \frac{\pi}{\sqrt{3}} Y$$

$$\text{when } \alpha = \frac{\pi}{2}$$

where P_0 = Minimum theoretical extrusion pressure

Y = Yield strength

d_1 = Initial bar diameter

d_2 = Final bar diameter

α = Half angle of die

μ_{db} = Coefficient of friction between die and billet

$C = \mu_{db} \cot \alpha$

Equations above consider only the friction between the die and the billet and not the friction between the container and the billet. Then considering the frictional effect between them, a following equation is obtained in Ref. (21):

$$P = P_0 e^{4\mu L/d_1} \approx P_0 (1 + 4 \mu_{cb} L/d_1)$$

where P = Maximum theoretical extrusion pressure

L = Length of bar before extrusion

μ_{cb} = Coefficient of friction between container and billet

The minimum and maximum theoretical pressure are

calculated using the equations above. By putting $\mu_{db} = 0.15$, $\mu_{cb} = 0.05$ taken from Ref. (5) $Y = 5.5$ MPa., $L = 70$ mm, $d_1 = 50$ mm and $d_2 = 25$ mm into the equations. Then, P_0 and P are obtained. These values are shown in Table 1.

TABLE 1. The Theoretical Extrusion Pressure

Half Angle	Maximum MPa	Minimum MPa
30	16	14
75	18	15
90	20	18

V. FLOW BEHAVIOUR DURING EXTRUSION

According to Pearson (23), flow behaviour can be categorized roughly into three types: type (a), which is obtained when extruding a homogeneous plastic material with little friction between the material and press tools; type (b) which is obtained when extruding homogeneous plastic material with a considerable amount of friction between the material and the press tools, type (c) which is obtained when extruding a nonhomogeneous material with, in general, a considerable amount of friction. These three types of flow are schematically illustrated in Fig. 8, from Unksov (24).

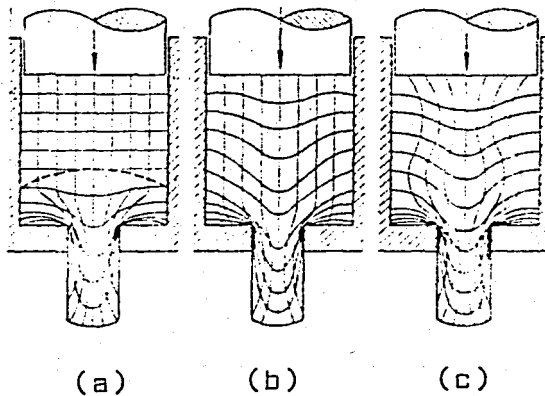


FIGURE 8- Schematic Representation of Three Different Types of Flow Behaviour During Extrusion (24).

(1) If the coefficient of friction is small, which is the case when the walls of the former are carefully machined and good quality lubrication is used, and there is no undue unevenness in the process of flow, caused by a large difference in temperatures of the tool (in particular the wall of the former) and the metal which is being formed, then the centre of deformation is near

to the die and comprises in height not more than half the diameter of the former (Figure 8-a). Flow patterns of this type occur during the lubricated extrusion of soft alloys such as lead, tin, α -brasses and tin bronzes, and in the extrusion of copper billets covered with oxide, which acts as a lubricant (1)

(2) For average values of the friction coefficient and when there is a certain difference in the temperatures of the former walls and the metal which is being formed, the centre of deformation extends over the whole height of the billet and the internal layers of the metal flow more intensely than the external layers (Figure 8-b). Flow type (b) is seen in single phase (homogeneous) copper alloys that do not form a lubricating oxide skin and in most aluminium alloys (1).

(3) With high values of the friction coefficient the presence of strong drag in the layers of metal adjoining the walls of the former, and also a considerable difference in the temperatures of the metal and the tool, three zones appear in the metal which is being formed characterizing the intensity of the flow. The first zone (Figure 8-c) is the internal zone of the metal placed directly opposite to the die, and has the highest intensity of flow. During movement of the pressplate, the metal of the second zone flows from the periphery to the centre and sets up constriction and a drop shaped arrangement in the first stage of the process there is minimum deformation, since the temperature of the metal in this zone will be at a minimum. This type of flow is found in the $(\alpha + \beta)$ -brasses, where the cooling of the peripheral regions of the billet leads to an increase in the flow stress, because the flow stress of the α phase is much higher than that of the β phase during hot working. As in the $(\alpha + \beta)$ -brasses, flow type (c) will occur when there is a hard billet

shell and, at the same time, the friction at the container wall is high. It can also occur without any phase change that leads to a higher flow stress if there is a large temperature difference between the billet and the container. This can take place in the extrusion of tin as well as of aluminum and its alloys. The extrusion defect known as pipe is caused by type (c) flow. It is an annular separation in the cross section at the rear of the extrusion. The non-uniform material flow in the container, together with the production and dissipation of heat, results in an uneven distribution of the strain rate, temperature and, therefore, the flow stress (1).

VI. DESIGN APPROACH TO FORWARD COLD EXTRUSION

A. Calculation of the Work of Deformation and the Extrusion Load

In practice, problems are usually solved by elementary analysis because it is easy to understand and simple to use. The solution obtained by elementary analysis has also proved to be most useful, because of its simplicity. Therefore this method is given priority.

1. Elementary Analysis

The starting point of this approach is the influence of the material, extrusion ratio, temperature and friction between the billet and the container on the magnitude of the work of deformation.

A considerable amount of calculation would be required to obtain the total work of deformation from the nonuniform distribution of strain and deformation energy in the deformation zone. Therefore, the billet is assumed to deform homogeneously with plane sections remaining plane. Tresca's yield criterion is used for the three-dimensional state of stress that develops in each element of volume under the applied ram load. Frictionless deformation of an element of volume by a change in length of dL requires the ideal deformation load F_{id} . The ideal work of deformation is:

$$dw_h = FdL$$

For uniaxial loading:

$$F = A_1 \cdot Y$$

which can be extended to:

$$F = \frac{V}{L} \cdot Y$$

giving:

$$dW_h = V \cdot Y \frac{dL}{L}$$

Therefore:

$$W_h = V \cdot Y \int_{L_1}^{L_2} \frac{dL}{L}$$

$$\int_{L_1}^{L_2} \frac{dL}{L} = \ln \frac{L_2}{L_1} = \ln \frac{L_2}{L_1} = \epsilon$$

The volume remains constant. Therefore:

$$A_2 L_2 = A_1 L_1$$

$$\ln \frac{L_2}{L_1} = \epsilon = \ln \frac{A_1}{A_2}$$

Hence:

$$W_h = V \cdot Y \cdot \epsilon$$

$$F_{id} = \frac{W_h}{L} = A_1 \cdot Y \cdot \epsilon$$

Where F_{id} is the ideal extrusion load. For the billets used in our studies:

$$F_{id} = A_1 \cdot Y$$

$$A_1 = \text{The initial cross section} = 1963.5 \text{ mm}^2$$

$$Y = \text{Yield strength} = 5.5 \text{ MPa}$$

$$\epsilon = \text{Strain} = \ln \frac{1963.5}{490} = 1.4$$

$$F_{id} = 1963.5 \times 5.5 \times 1.4 = 15,000 \text{ Newtons.}$$

However, additional work W_i is required, over and above the

homogeneous work of deformation, to overcome the shearing deformation-redundant work-in the deformation zone (and friction at the die), as well as the work W_f needed to overcome the friction between the billet and the container, or to shear the material close to the billet surface if sticking friction occurs:

$$W_a = W_h + W_i + W_f$$

W_i is difficult to determine theoretically, and so it is combined with W_h , and the efficiency of the deformation is defined as:

$$\eta = \frac{W_h}{W_h + W_i}$$

which can be measured and which enables the redundant work to be allowed for empirically.

The following expression is then obtained:

$$W_h + W_i = \frac{W_h}{\eta} = V \cdot \epsilon \cdot \frac{Y}{\eta}$$

The term Y/η is known as the deformation resistance. It differs from the yield strength Y , which is a material constant, inasmuch as it includes the internal shearing losses that depend on the geometry of deformation and the die friction. The additional work that has to be expended to overcome the friction between the billet surface and the container is:

$$W_f = \pi \cdot d_1 \cdot L_1^2 \cdot \mu_{cb} \cdot Y$$

The expression for the total work then becomes:

$$W_a = V \cdot \epsilon \cdot Y_w + \pi \cdot d_1 \cdot L_1^2 \cdot \mu_{cb} \cdot Y$$

and the total load is given by:

$$F_a = A_1 \cdot \epsilon \cdot Y_w + \pi \cdot d_1 \cdot L_1 \cdot \mu_{cb} \cdot Y$$

The efficiency factor η , according to the Ref. (30), is generally between 0.3 and 0.8. The coefficient of friction at the container wall can vary considerably, depending on the alloy and the lubricant. At temperature close to room temperature and with good lubrication, it can vary from 0.05 to 0.15. In nonlubricated extrusion, it varies from 0.35 to 0.45 (5).

For the billets used in our studies:

$$F_a = A_1 \cdot \epsilon \cdot Y_w + \eta \cdot d_1 \cdot L_1 \cdot \mu_{cb} \cdot Y$$

Where A_1 = The initial cross section = 1963.5 mm²

$$\epsilon = \text{Strain} = \ln \frac{1963.5}{490} = 1.5$$

Y = Yield strength = 5.5 MPa.

η = Efficiency factor = 0.7, taken from Ref. (30)

$$Y_w = \text{Deformation resistance} = \frac{5.5}{0.7} = 7.9 \text{ MPa.}$$

d_1 = The initial bar diameter = 50 mm.

L_1 = Length of bar before extrusion = 70 mm.

μ_{cb} = Coefficient of friction between container and billet = 0.05, taken from Ref. (5)

$$F_a = 1963.5 \times 1.4 \times 7.9 + 50 \times 70 \times 0.05 \times 5.5 = 25,000 \text{ Newtons.}$$

B. Design of Containers with Round Bores

Containers are most expensive of all extrusion tooling because of the large volume of steel needed. The efficiency of the extrusion process depends to a very high degree on the durability of the container.

Calculations are indispensable to obtain the correct dimension of the container components and to choose the most suitable steels. Axial deformation forces act on the stem and die during extrusion. On the other hand, radial forces act on the container as tangential and radial stresses σ_θ and σ_r .

which can have very high values. The only axial stresses in the container come from the friction between the billet and the inner surface of the container. The theory of thick-wall cylindrical vessels under internal pressure is used to calculate the individual stresses in the container. The equations for the radial and tangential stresses at any arbitrary point in the hollow body can be determined as a function of the pressure and the dimensions from the equilibrium of forces and the relationships between stress and strain. For a hollow body subjected to an internal pressure:

$$\sigma_r = P_{ri} \frac{d_i^2}{d_a^2 - d_i^2} \left\{ 1 - \frac{d_a^2}{d^2} \right\}$$

$$\sigma_\theta = P_{ri} \frac{d_i^2}{d_a^2 - d_i^2} \left\{ 1 + \frac{d_a^2}{d^2} \right\}$$

where,

σ_r = Radial stress

σ_θ = Tangential stress

P_{ri} = Internal radial pressure

d_i = Inside diameter of the container bore

d_a = Outside diameter of the container

The stress variation across the container wall is, therefore, hyperbolic and the peak stress—the maximum stress—always occur at the inner wall of the hollow body regardless of whether the pressure is applied internally or externally. The initial assumption is that the container is only stressed in two dimensions and, accordingly, the effect of the stresses must be combined into a resultant stress σ_R . The resultant stress implies that flow occurs only in a continuous medium stressed in several dimensions when σ_R exceeds the flow stress determined from uniaxial tensile tests (1).

The maximum strain criterion was previously used to calculate the equivalent stress σ_R in container calculations. However, experiments have indicated that the strain hypothesis considerably underestimates the danger of fracture (1). The strain energy hypothesis gives better agreement with the initiation of plastic deformation under multiaxial stresses for materials, including the hot working steels, generally used for container construction. According to this criterion, under a two-dimensional stress system-e.g., the principal stresses σ_r and σ_θ -flow occurs when

$$\sigma_R = \sqrt{\sigma_\theta^2 + \sigma_r^2} - \sigma_\theta = \sigma_r = Y$$

A safety factor is usually introduced into the calculations :

$$\sigma_R \cdot S < Y$$

where the safety factor S should normally be between 1.15 and 1.3 (1)

1. Design of Monobloc Containers

In this case the liner and mantle are the same components. Therefore the high stress peaks on the inner wall during extrusion restrict the load carrying capacity compared to a compound container. The extrusion pressure induces tensile tangential stresses internally and externally and the inner wall is also subjected to compressive stresses. The maximum stresses resulting from the extrusion pressure occur at the bore and the minimum at the outer surface. At the internal wall:

$$\sigma_r(d_i) = \sigma_{rmax} = P_{ri} \frac{d_i^2}{d_i^2 - d_a^2} \left\{ 1 - \frac{d_a^2}{d_i^2} \right\} = P_{ri}$$

$$\sigma_{\theta}(d_i) = \sigma_{\theta \max} = P_{ri} \frac{d_i^2}{d_a^2 - d_i^2} \left\{ 1 + \frac{d_a^2}{d_i^2} \right\} = P_{ri} \frac{u+1}{u-1}$$

Where $u = \text{diameter ratio} = d_a/d_i$

At the external wall:

$$\sigma_r(d_a) = \sigma_{r \min} = P_{ri} \frac{d_i^2}{d_a^2 - d_i^2} \left\{ 1 - \frac{d_a^2}{d_a^2} \right\} = 0$$

$$\sigma_{\theta}(d_a) = \sigma_{\theta \min} = P_{ri} \frac{d_i^2}{d_a^2 - d_i^2} \left\{ 1 + \frac{d_a^2}{d_a^2} \right\} = P_{ri} \frac{2}{u-1}$$

The working pressure P_{ri} at the inner liner wall of the container was taken to be less than the full specific pressure P_s because there is no hydrostatic stress distribution in the container. Metallic materials do not behave as a fluid even when they are very plastic. As well as being dependent on the deformation resistance of the individual alloys, the radial pressure is also a function of the friction between the billet and the container liner. The radial pressure P_{ri} decreases with increasing friction. Usually, P_{ri} is taken to be 0.6 to 0.8 P_s , with the maximum radial pressure being used for the design of the containers for alloys extruded with little friction between the billet and the container and vice versa.

For the container used in this study a 48 CrMoV 67 type of steel was chosen, alloy number 1.2323, heat treated to 1300 MPa, with a hardness of 50 HRC.

$$\sigma_R = \frac{1300}{1.25} = 1040 \text{ MPa.}$$

$$\text{The specific pressure is } = \frac{3 \times 10^5 \times 4}{\pi \times 5^2 \times 10^2} = 153 \text{ MPa.}$$

and $P_{ri} = 0.8P_s = 123 \text{ MPa}$.

At the Internal wall:

$$\begin{aligned}\sigma_r(d_i) &= -123 \text{ MPa.} \\ \sigma_\theta(d_i) &= 123 \frac{u^2+1}{u^2-1}\end{aligned}$$

At the external wall:

$$\begin{aligned}\sigma_r(d_a) &= 0 \\ \sigma_\theta(d_a) &= 123 \frac{2}{u^2-1}\end{aligned}$$

Therefore the equivalent stress at the internal container wall is:

$$1040^2 = \sigma_\theta^2 + \sigma_r^2 - \sigma_\theta \cdot \sigma_r$$

$$1081600 = 15129 \left(\frac{u^2+1}{u^2-1} \right)^2 + 15129 + 15129 \left(\frac{u^2+1}{u^2-1} \right)$$

By putting $t = \frac{u^2+1}{u^2-1}$, the above equation becomes,

$$t^2 + t - 72 = 0$$

which has the solution $t=8$, from which the outside diameter $d_a = 57.5 \text{ mm}$ is found.

C. Stems for Rod Extrusion

The design of extrusion stems varies according to the size, shape and operating stresses. Frequently, the rigidity of the stem is the factor that determines the specific pressure that can be applied during extrusion. The value of 1100 MPa. generally should not be exceeded but much higher pressures are found in production. Pressures up to 1350 MPa are now used for zinc alloys, difficult aluminium alloys, and for nickel alloys and steels (1).

D. Dies for Forward Cold Extrusion

The element of cold forward extrusion die are shown in Figure 9. The bar is forced into the conical portion of the die. In this conical area, the bar goes from its initial elastic state to a plastic state during which the metal can flow. This area is labelled "plasticized zone". After the plasticized zone, the metal enters the die orifice in which the bar assumes its final shape. The actual deformation of the bar takes place in the plasticized zone. In the die orifice, the metal returns to an elastic state. The final cross section of the bar is determined by the shape of the die orifice. Dies can be made either from tool steel or tungsten carbide. Steel dies must have a minimum hardness of 55 R.C. Carbide dies are usually made as inserts inside a casing (25).

The primary criterion in die material selection is the number of parts to be made. Carbide dies are most costly and difficult to make than steel, but last much longer. As many as 250,000 parts can be extruded from a properly designed carbide die (25).

The geometric variables in forward cold extrusion is shown in Fig. 10. These are: the initial bar diameter (d_1), the final bar diameter (d_2), the included die angle (θ) and the die land length (l).

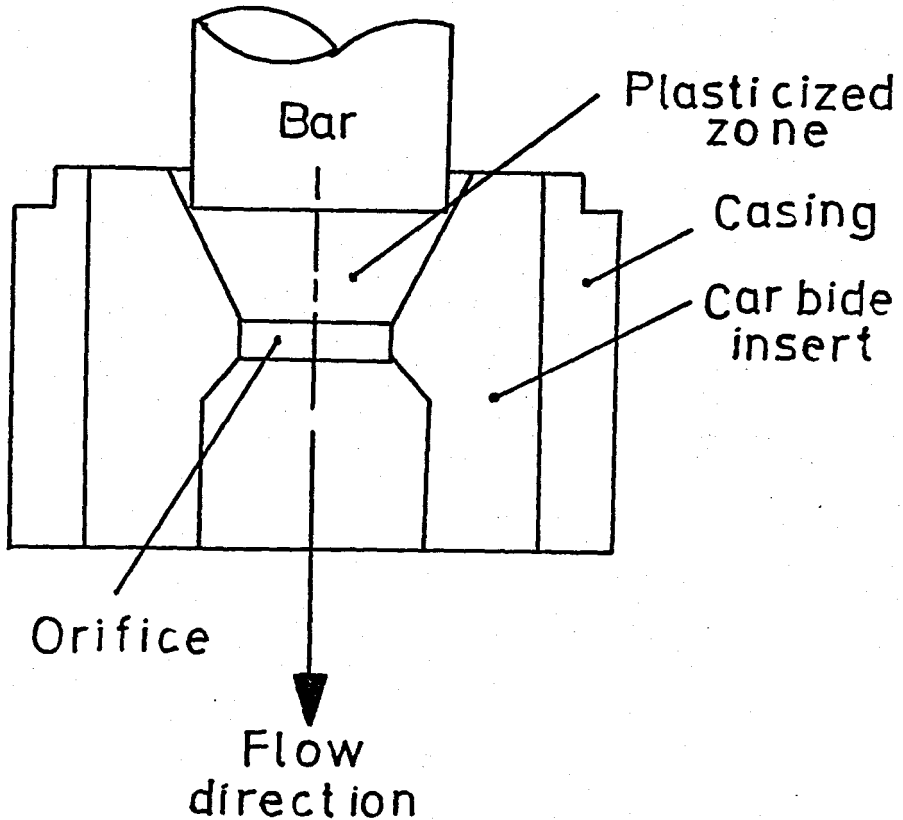


FIGURE 9- The Major Features of a Cold Extrusion Die Can Be Seen in This Carbide Die Cutaway. Note the Insert-Inside-Casing Construction of the Die, the Plasticized Zone Where Deformation Takes Place, and the Orifice That Determines the Shape of the Extruded Bar (27).

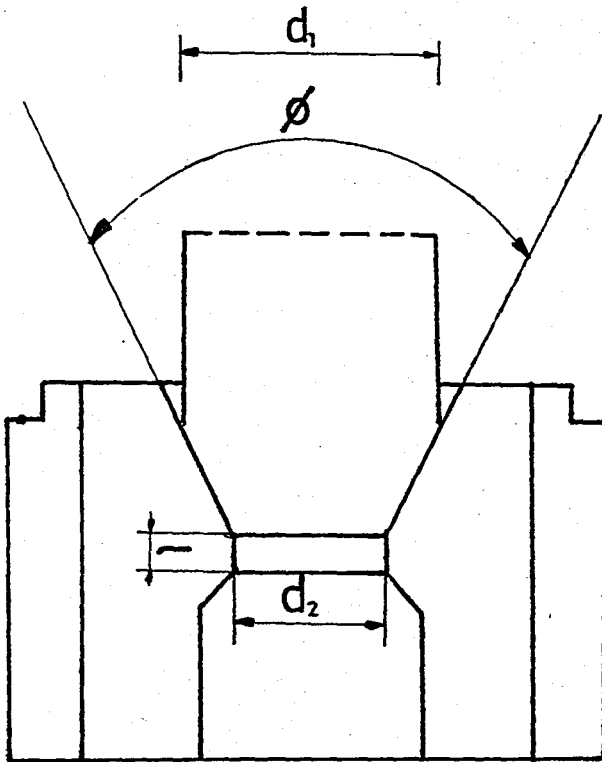


FIGURE 10- The Geometric Variables in Forward Cold Extrusion are Shown. They are: the Initial Bar Diameter (d_1), the Final Bar Diameter (d_2), the Included Die Angle (ϕ) and the Land Length (l) (27).

VII. EXPERIMENTAL TECHNIQUE AND RESULTS

A. Extrusion Equipment and Billet Preparation

The billets used in these studies were 50 millimeters in diameter by 70 millimeters long. The billets were extruded with reduction of 75 per cent of the cross-sectional area. The size of the extruded bars and the extrusion ratio corresponding to this reduction are as follows:

<u>Reduction in area,</u> <u>percent</u>	<u>Area of cross-section,</u> <u>mm²</u>	<u>Diameter</u> <u>mm</u>	<u>Extrusion</u> <u>Ratio</u>
Initial billet	1963.5	50	..
75	490	25	4.00:1

To study the effects of die design, conical-shaped dies having included angles of 60, 150 and 180 deg. were used for the same reduction. Also, to study the effects of lubricants, LM22 MoS₂-pulverspray, Pure Vaseline and Lanoline were used.

The extrusion test were performed on a 50 ton hydraulic press. The press, similar to those in use for cold-extruding aluminium, is equipped with a die cushion that has a 80 ton stripping capacity. The tools consists of a punch, container, interchangeable dies and holder. A photo of the complete tool assembly is shown in Fig.11.

As the experimental arrangements are shown in Fig. 12, they can be divided into two parts, that is, an extrusion apparatus and some lubricants.

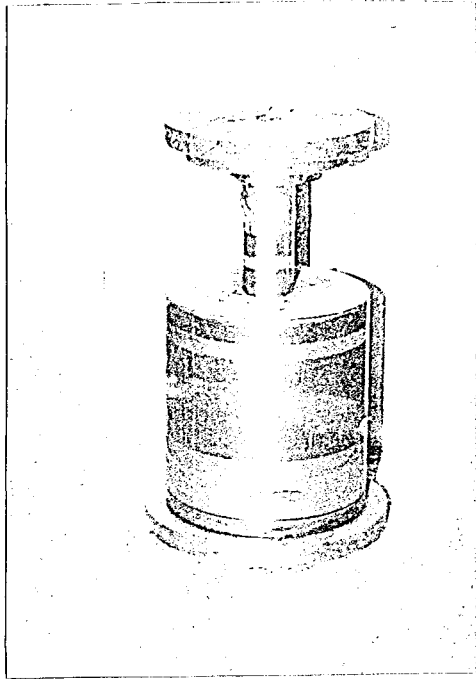


FIGURE 11- Extrusion Apparatus

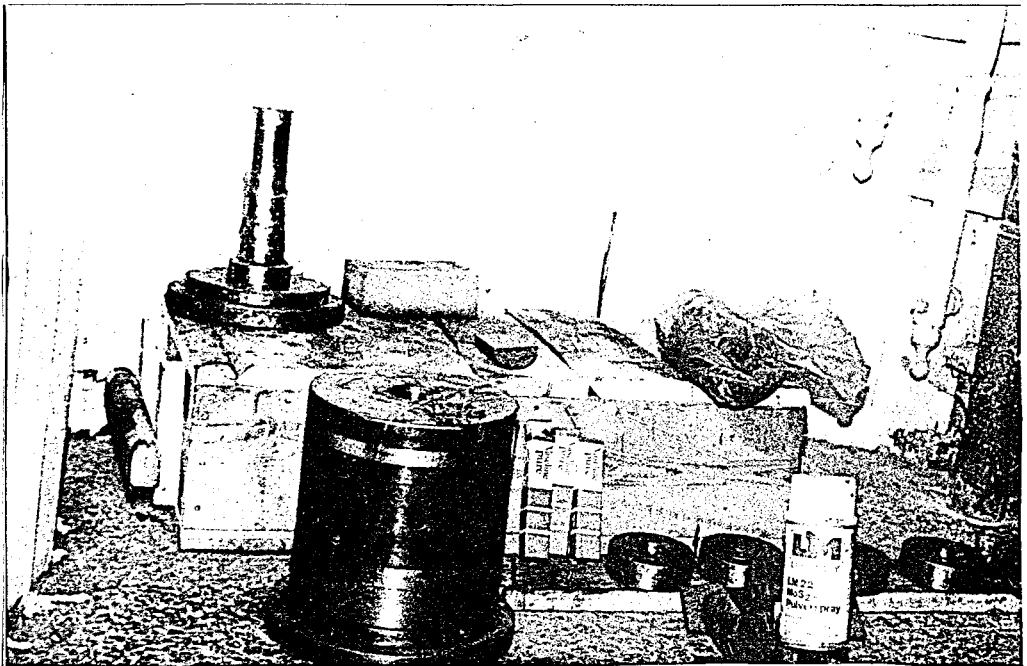


FIGURE 12- Experimental Arrangements.

1. Extrusion Apparatus

This apparatus is able to extrude directly a billet which has the diameter of 50 mm.

a. Dies

As shown in Fig. 13 the diameter of billet changes from 50 millimeters to 25 millimeters through the die, therefore the reduction is 75 per cent.

b. Container

This container can extrude a billet whose diameter is 50 millimeters.

The technical drawings of the extrusion apparatus are given in the Appendix.

Extrusion billets were prepared from lead alloy including Sn:1.4 per cent, Sb: 0.3 per cent. The engineering stress, and the true stress in compression for this lead are both plotted against strain in Fig. 14 (7). Billet stock was assured in the form of casting. The bar was casted, as shown in Figure 15.

The approximation was made from Ref. (28) for the mechanical properties of the commercial lead, which was used in our experiments.

Ultimate strength,.....	17.5 MPa.
Yield Strength,.....	5.5 MPa.
Elongation, per cent in 50 mm.....	4.0
Hardness, Bhn (5×10^3 N)	4.9
Modulus of elasticity	2.1×10^5 MPa.

Split billets for the studies on metal flow were prepared only from commercial lead. The meridian plane of the sectioned was provided with a machined square grid network spaced 5.0 millimeters apart and a line depth of 0.2 millimeters, as shown in Fig. 16.

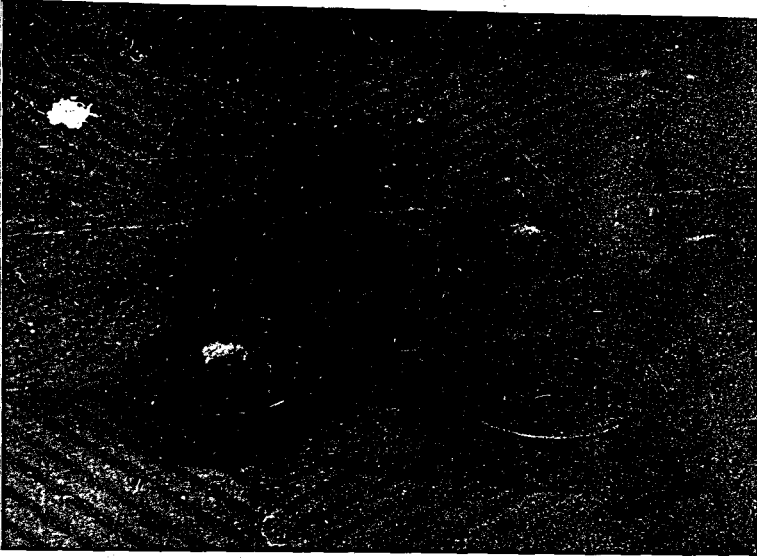


FIGURE 13- Dies for Cold Extrusion of Solid Round Bars.

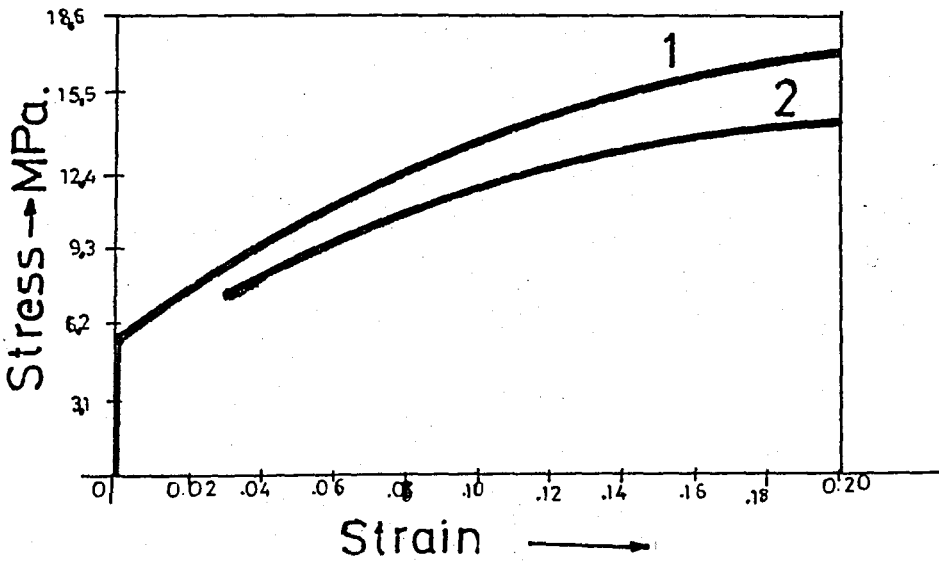


FIGURE 14- Stress-Strain Curves for Lead in Compression.
1. Engineering Stress. 2. True Stress (7)

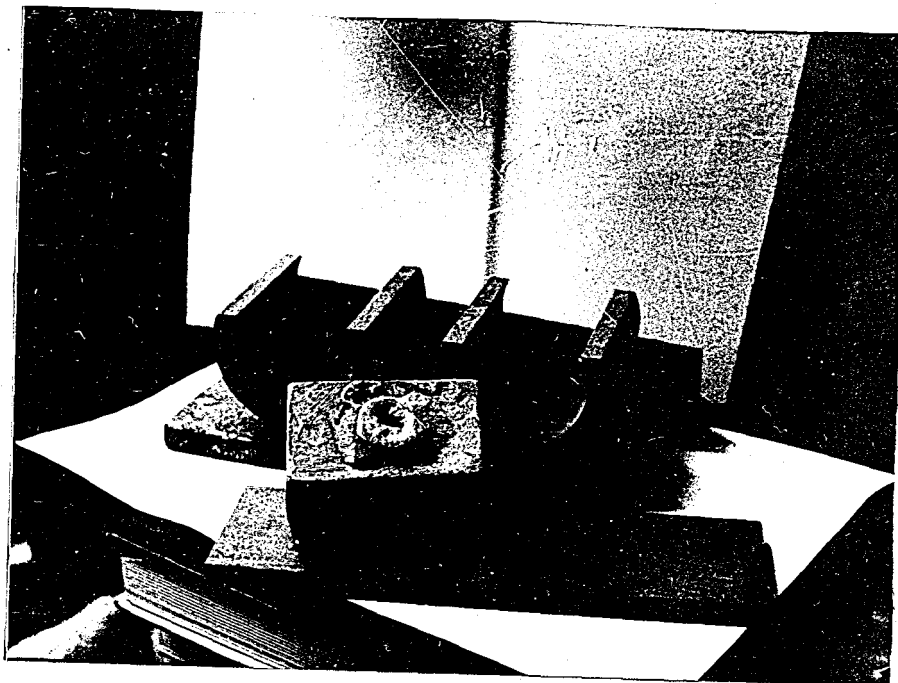


FIGURE 15- Casting Mold and Billet.

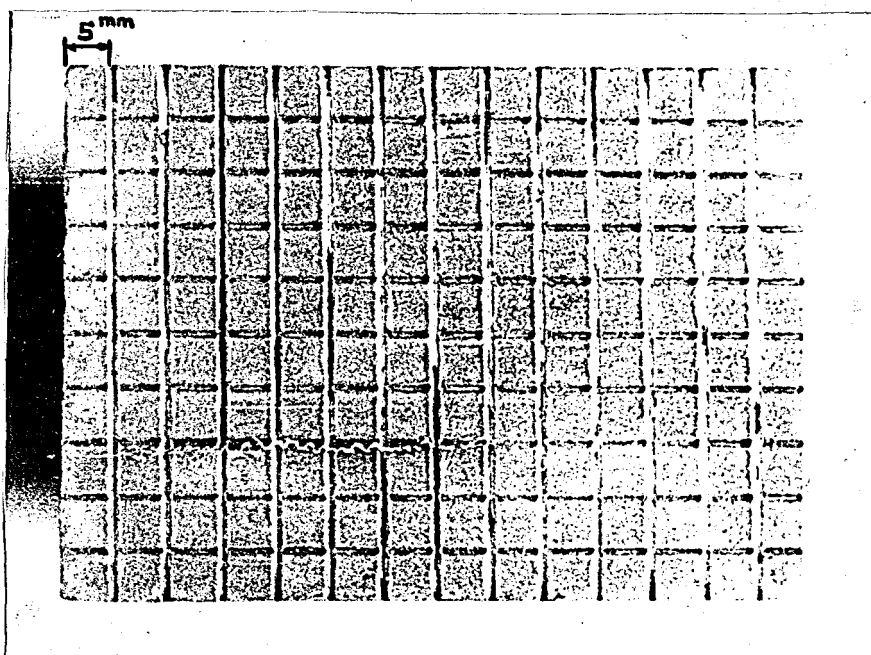


FIGURE 16- Sectioned Billet Which is Machined Square Grid Network Spaced 5.0 millimeters Apart and a Line Depth of 0.2 millimeters.

B. Heat Treatment and Lubrication

Each half of the split billets were placed in furnace set for 250°C . A 15 minutes soak period starts when thermocouple reaches 205°C (Approximately $1-\frac{1}{2}$ hour cycle).

C. Description of Extrusion Tests and Results.

The split billets could be extruded easily with a 75 per cent reduction, but the extruded bar could not be ejected from the die. Therefore, as shown in Figure 17, the split billets were cut into two parts.

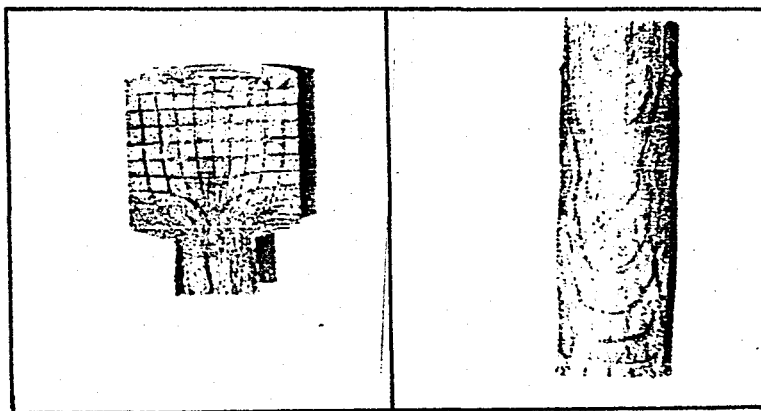
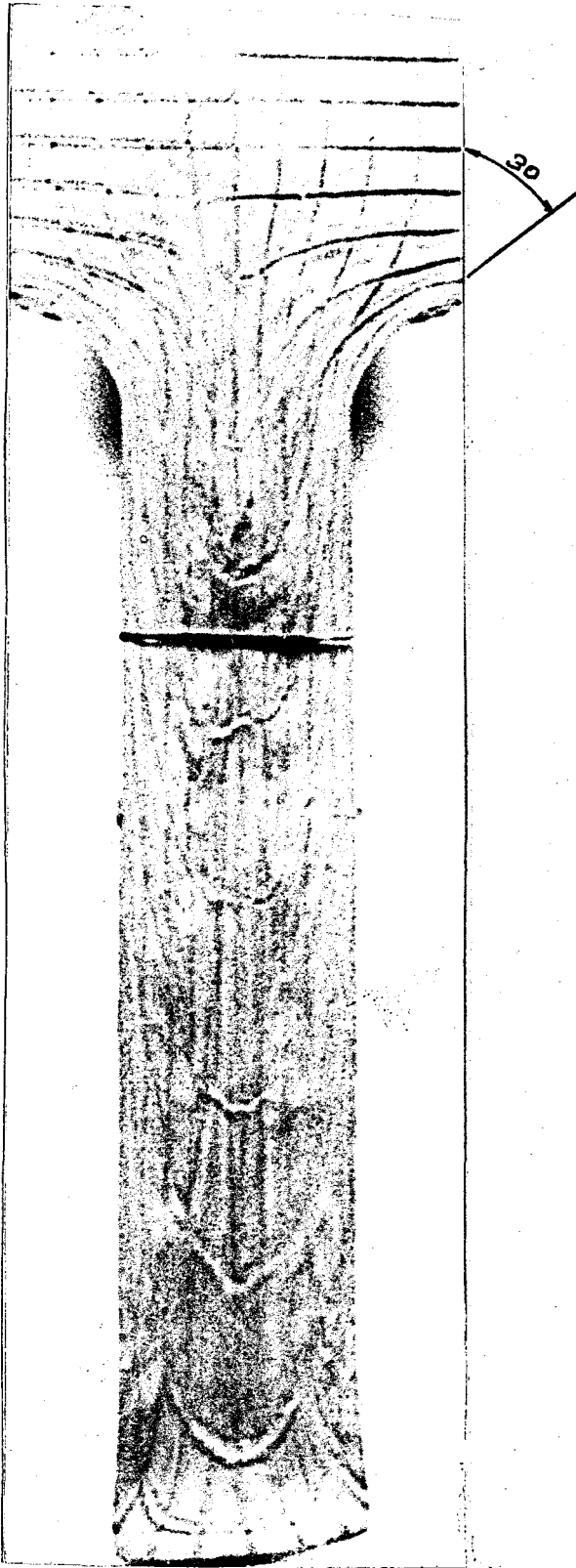


FIGURE 17- Cut Split Billet.

Photographs of the split billets extruded with a reduction of 75 per cent through 60, 150 and flat (180) dies, after removal of the lubricant are shown in fig. 18, 19 and 20. When the flow patterns shown in the Figures are compared with the schematic representation of three different types of flow behaviour during extrusion given in Fig. 8, it is recognized that the results, we have obtained from our experiments match the flow in type (a). The main features are as follows. In all cases the billet has undergone no deformation until fairly close to the die opening. Thus, the plastic deformation is restricted to a fairly localized region in the neighbourhood of the dies. Secondly, the

material is severely dragged back along the chamber walls, and a "dead" metal region forms under the shoulders of the dies.

The billets were extruded at a speed of 2.50 mm/sec. (measured as punch speed). The low speed used in these studies was selected to avoid damage to the tools. Good surface finishes were obtained on the split billets, indicating that the LM22 MoS₂-Pulverspray, Pure Vaseline and Lanoline were effective in preventing seizing. Any surface imperfections found on the split billets were caused by chattering during ejection.



Lubricant:

Lanoline=2.0 kg

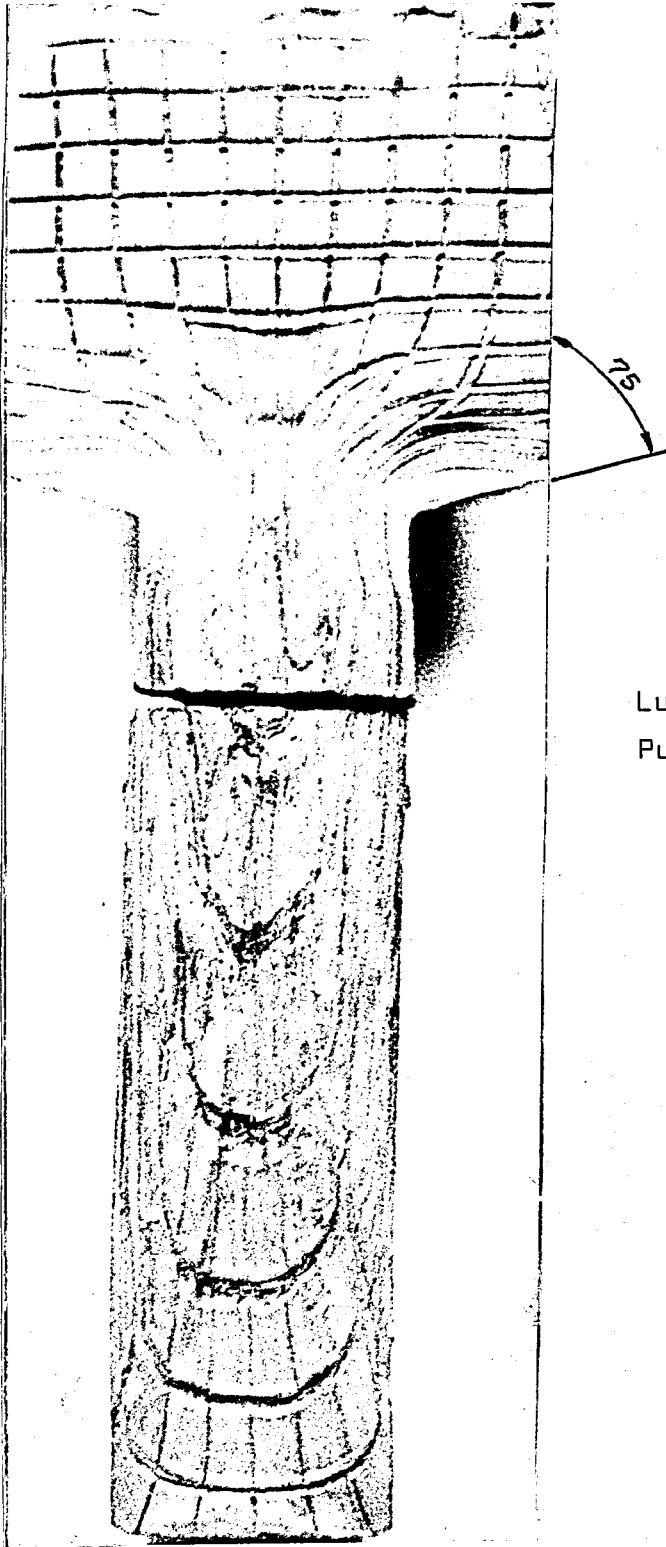
Cylinder oil=1.1 kg

Animal fat=0.2 kg

Glycerol=0.03 kg

Carbon tetrachloride=10 Lt

FIGURE 18- Commercial Lead Alloy Split Bar Extruded with a 75 Per Cent Reduction through 60-Deg Die.



Lubricant:
Pure Vaseline

FIGURE 19- Commercial Lead Alloy Split Bar Extruded with a 75 Per Cent Reduction through 150-Deg Die.

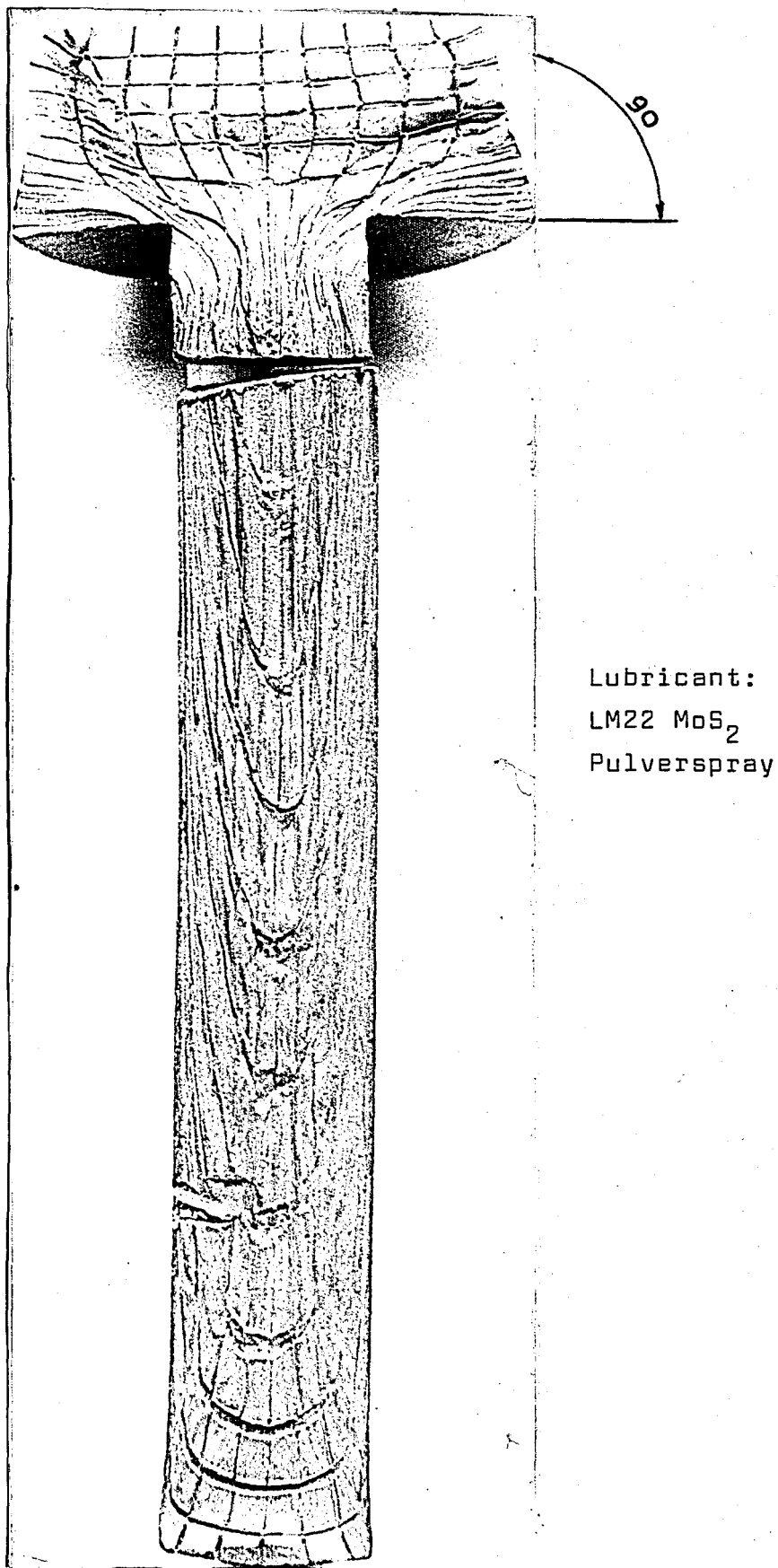
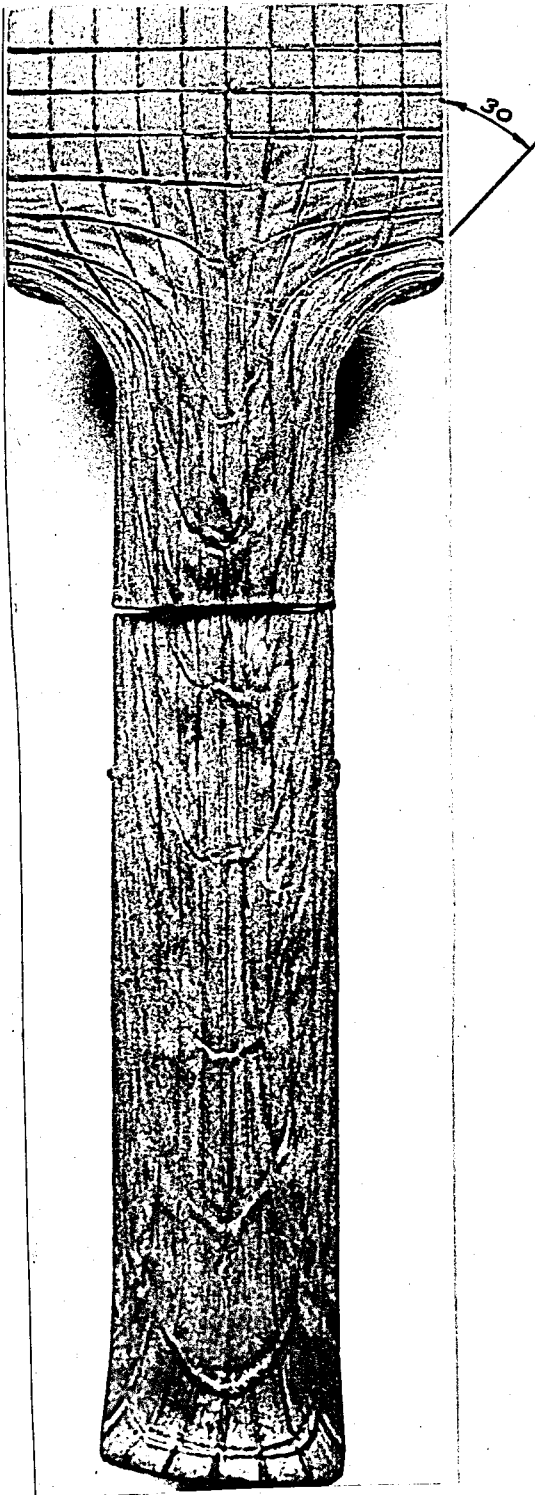


FIGURE 20- Commercial Lead Alloy Split Bar Extruded with a 75 Per Cent Reduction through 180 (Flat)-Deg Die

VIII. METAL FLOW DURING EXTRUSION

Sections of the split billets extruded with 75 per cent reduction through the 60, 150 and 180-deg. dies showing the distortion of the inscribed grids, are presented in Fig. 21, 22 and 23. An examination of Figures shows, during the initial stage of extrusion, the core of the billet advances into the die with practically no deformation taking place, whereas the peripheral fibers undergo severe axial compression. As the billet begins to extrude, the flow becomes markedly nonuniform because of the action of shear stresses on the outer fibres. Along the axis of the bar (central grid zones), deformation occurs principally as simple elongation (and compression) with a slight amount of shear. The outer grid zones undergo an equal amount of elongation, but are also subjected to additional shear deformations, which increase in magnitude toward the bar surface. Because of the friction at the surface of the die, the radial flow of the peripheral zones is retarded and the amount of shearing in this region is increased. Thus, the total deformation of the outer fibers is greater than at the axis. As shown in Figure 24, This fact is clearly apparent from the lengths of the third transverse grid-line units at the bottom in the outer and central grid zones are compared.

The grid spacings in the bars extruded with a 75 per cent reduction were the same for the 60, 150 and 180-deg die angles. For the same reduction, the influence of the die angle on deformation pattern in the extrusion tests is shown in Fig. 25.



Lubricant:

Lanoline= 2.0 kg

Cylinder oil=1.1 kg

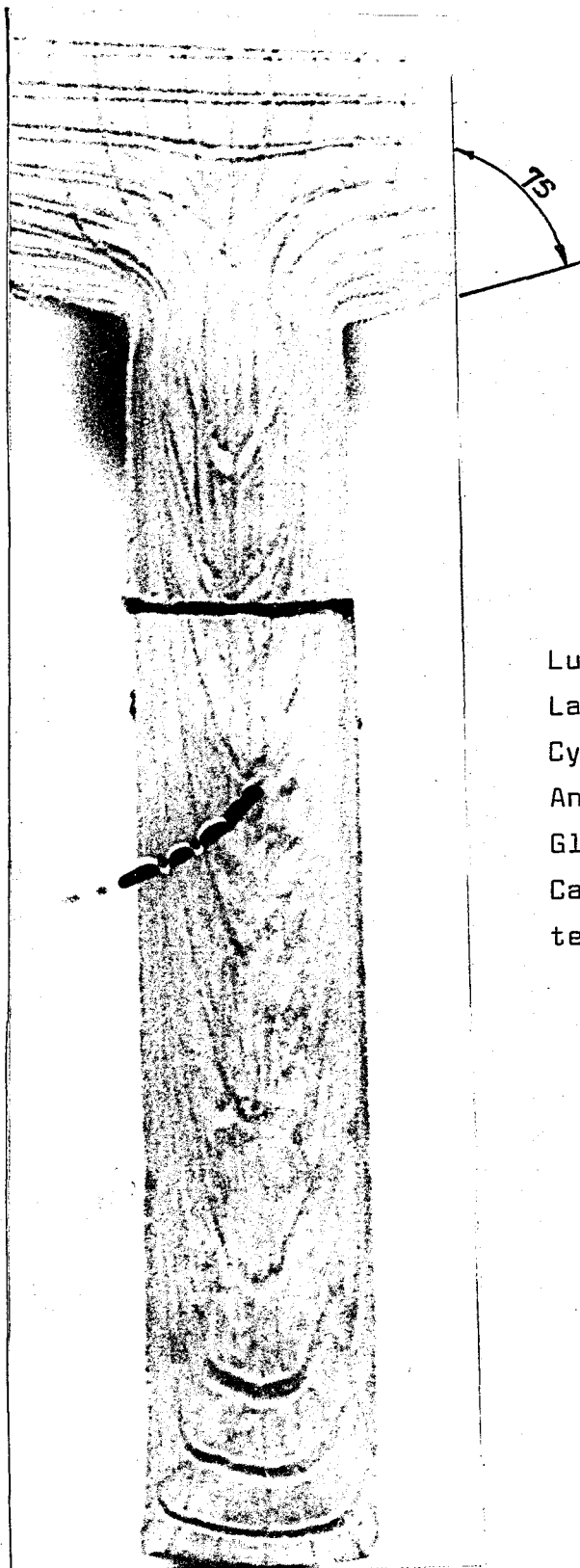
Animal fat= 0.2 kg

Glycerol = 0.03 kg

Carbon

tetrachloride=10 lt

FIGURE 21- Deformation Pattern, during Direct Extrusion of Square Grid Network on Meridian Plane of Lead Billet.



Lubricant:

Lanoline= 2.0 kg

Cylinder oil = 1.1 kg

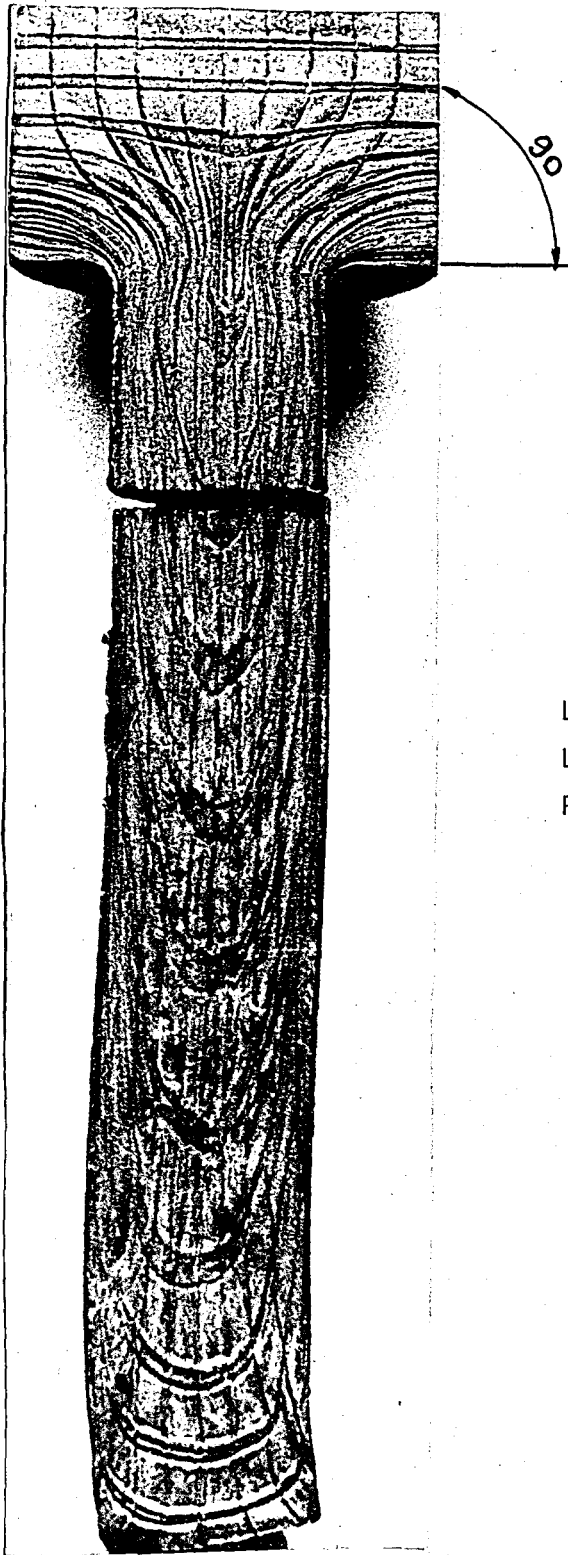
Animal fat= 0.2 kg

Glycerol= 0.03 kg

Carbon

tetrachloride= 10 Lt

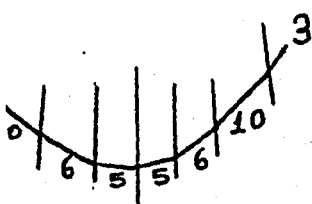
FIGURE 22- Deformation Pattern, during Direct Extrusion of Square Grid Network on Meridian Plane of Lead Billet.



Lubricant:
LM22 MoS₂
Pulverspray

FIGURE 23- Deformation Pattern, during Direct Extrusion of Square Grid Network on Meridian Plane of Lead Billet.

Lubricant:
Pure Vaseline



The third
transverse
grid-line

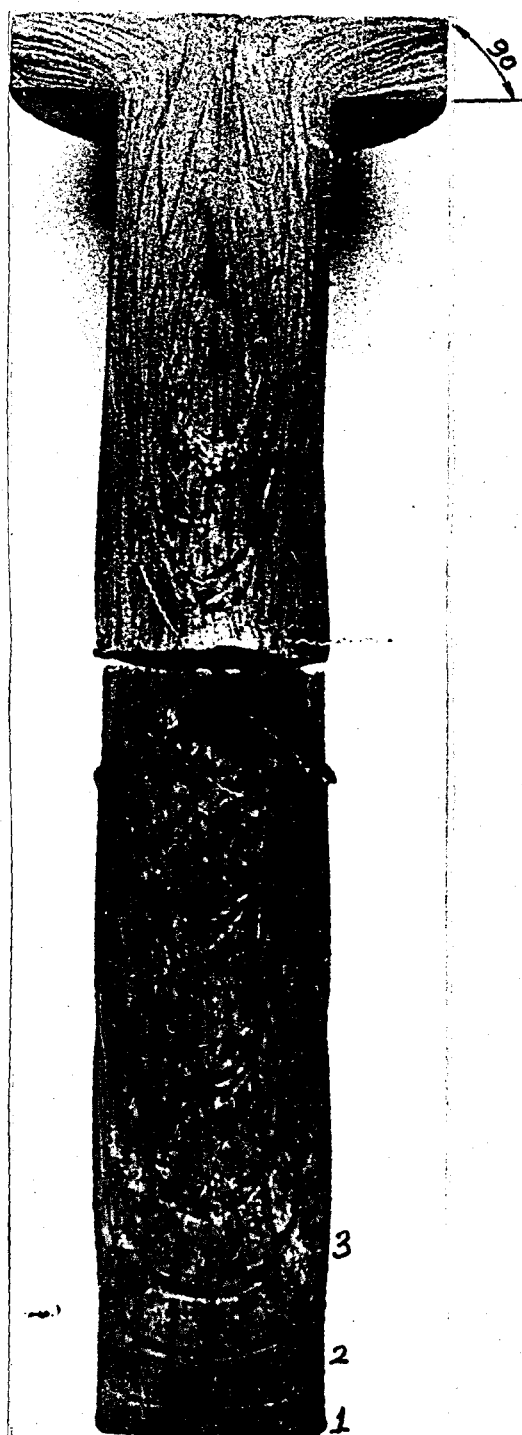


FIGURE 24- Experimentally Observed Flow Pattern in Commercial Lead Alloy Extruded at Room Temperature and Ram Speed of 2.5 mm/sec.

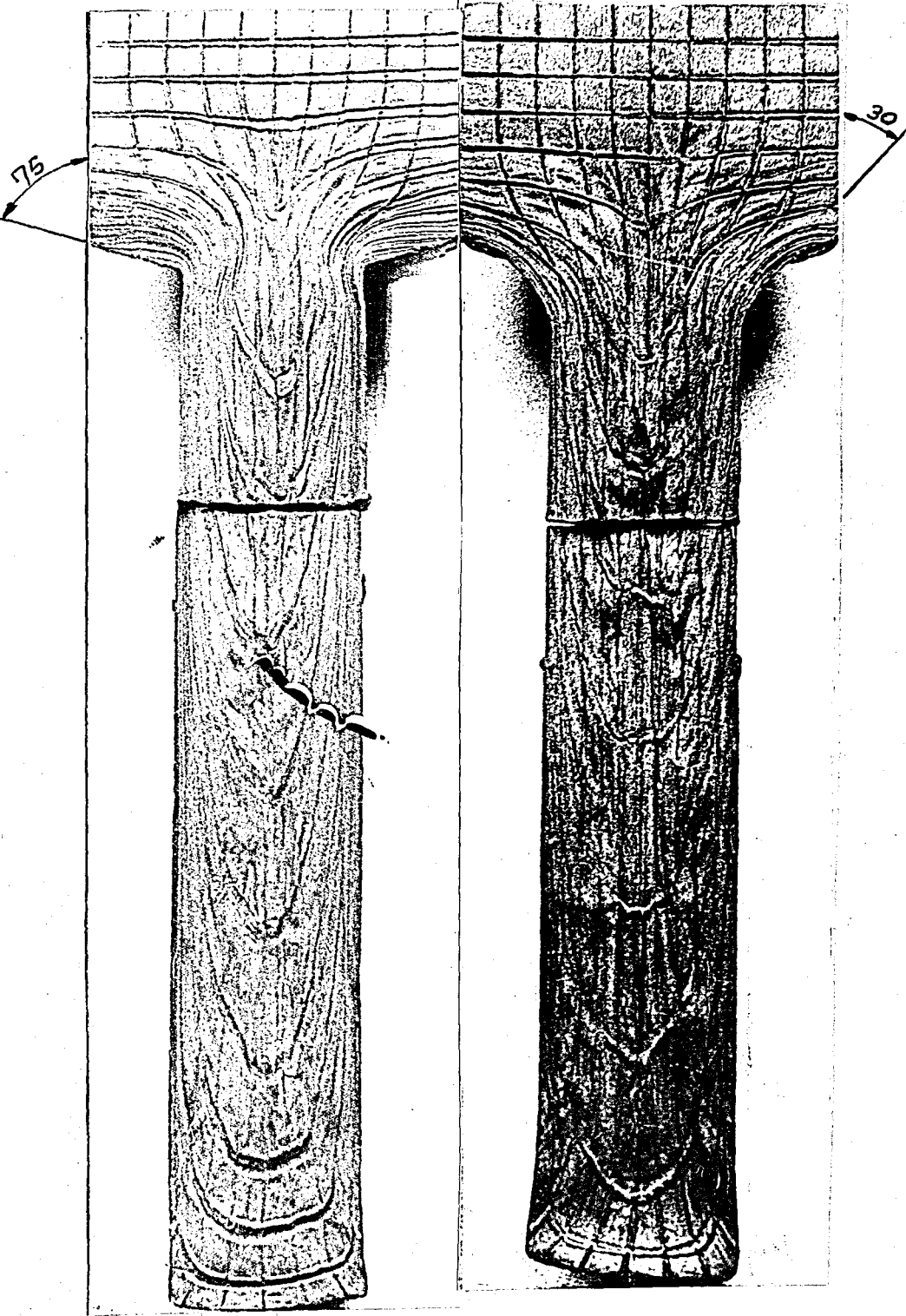


FIGURE 25- Deformation Pattern, During Direct Extrusion of Square Grid Network on Meridian Plane of Lead Billet.



Lubricant:

Lanoline= 2.0 kg

Cylinder oil =1.1 kg

Animal fat= 0.2 kg

Glycerol=0.03 kg

Carbon

tetrachloride= 10 Lt

FIGURE 26- Deformed Grid Network of Commercial Lead Alloy after Extrusion.

An examination of the figure shows for the same transverse grid line (see fifth and sixth transverse grid lines from the top of both photographs), the concavity being in the extrusion direction started earlier for the larger die angle. For the same reduction, the shear displacement of the transverse grid lines increased as the die angle increased. The increase in displacement takes place almost completely within the outermost grid zones. Thus, it was apparent that, for a given reduction, the principal effect of the die angle on the deformation process is in the outer fibers of the metal.

In addition, the following observation was made from measurements of the grid spacings in the extruded bars; except for the initial flow portion, as shown in Fig. 26 the grid zones were uniformly compressed and elongated over the cross-section of the bar. An examination of the same Figure shows the longitudinal and transverse lines of the network remain approximately equidistant after extrusion (except for the end effects in the extruded material).

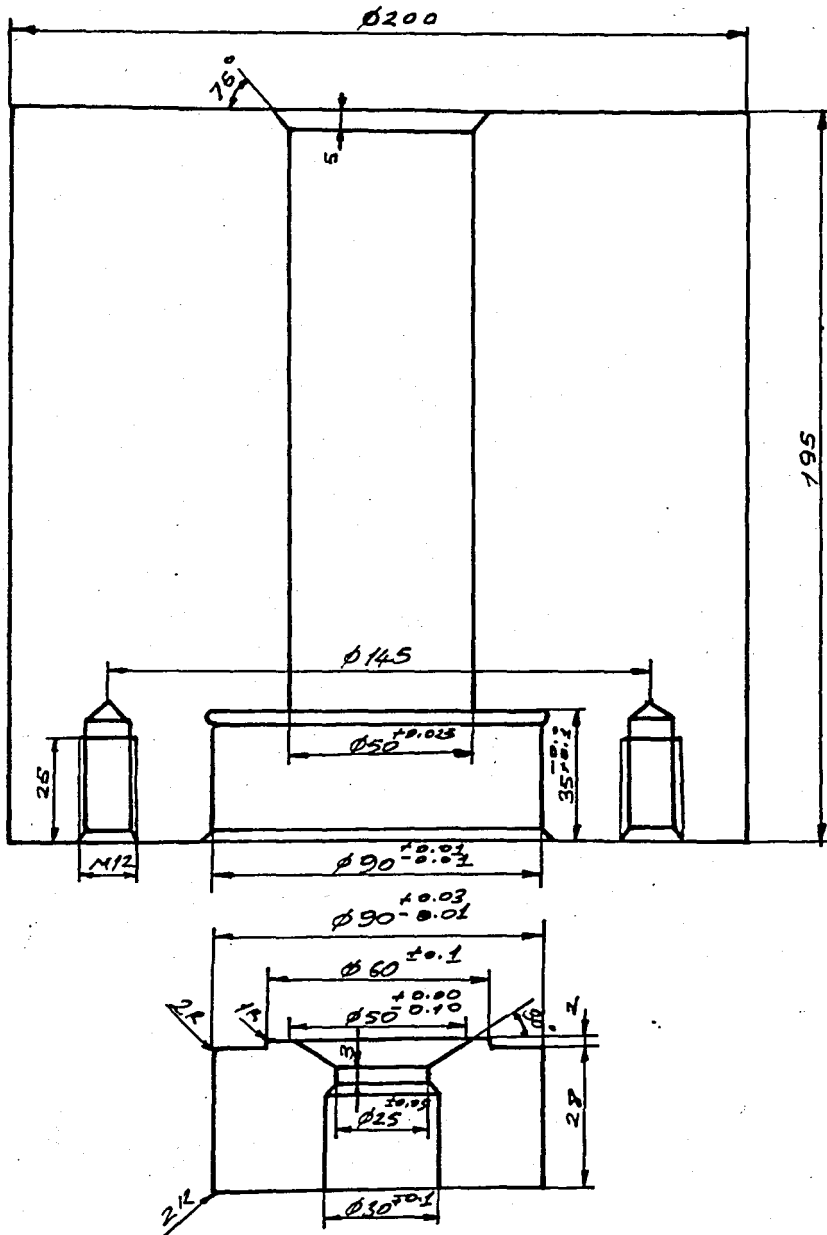
In Fig. 26, for the half angle of 30° , the grid distortion reveals no "dead corner". The criterion of the existence of the dead corner seems still a mystery. It must have close relations with parameters such as extrusion ratio, die angle, surface friction, extrusion speed, and die entry radius. Any further work along this line will be a contribution of foremost importance to the field of extrusion.

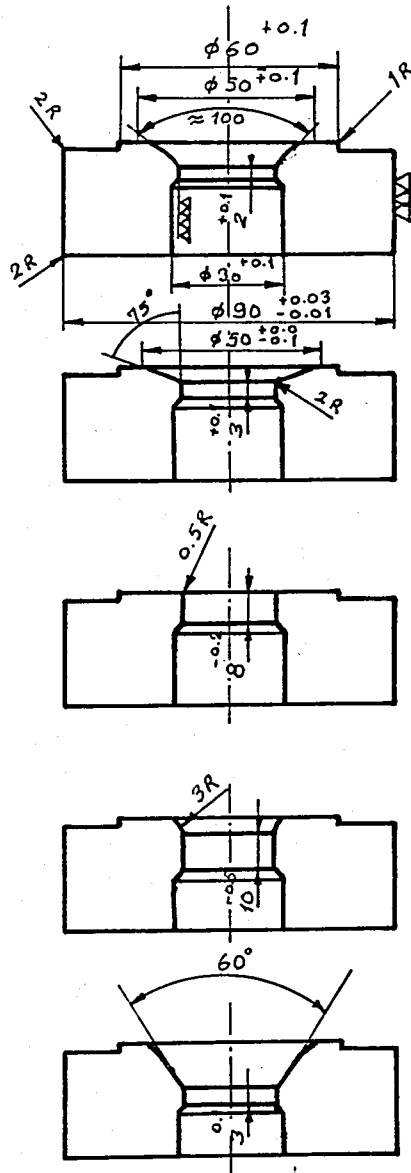
IX. CONCLUSIONS

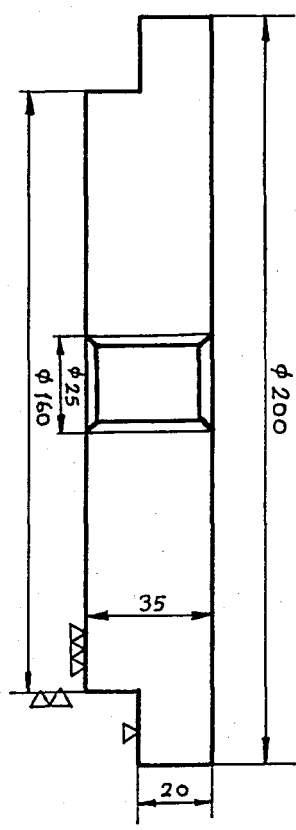
1. Metal flow during extrusion of commercially pure lead at various die angles (60 , 150 , 180) is found to be of type (a) as expected for soft alloys.
2. LM22 MoS₂-Pulverspray, Lanoline and Pure Vaseline were effective in preventing seizing between the workpiece and the die land length in producing good surface finish.
3. The main deformation takes place in the outer layers of the extruded section
4. The degree of deformation increases with increasing die angle.
5. The surface quality of the extruded shape depends on the quality of the surface of the billet from which it is pressed. A defect originally located in the surface of the billet will appear on the surface of the extrusion.

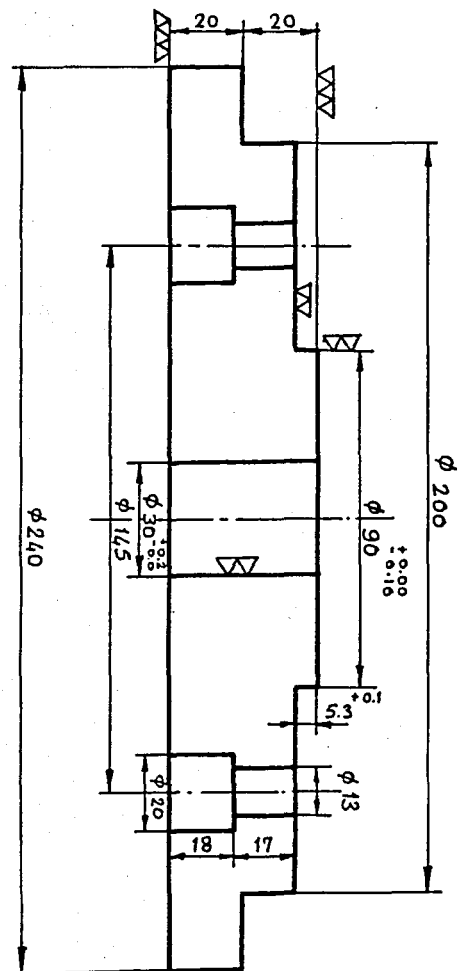
APPENDIX

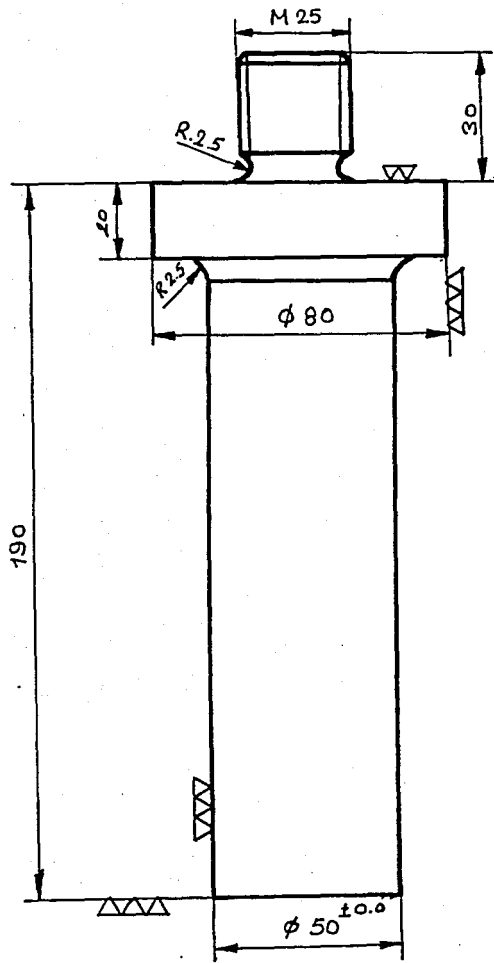
TECHNICAL DRAWINGS OF THE EXTRUSION APPARATUS
INCLUDING CONTAINER, DIES, HOLDERS AND PUNCH
FOR COLD EXTRUSION OF SOLID ROUND BARS











BIBLIOGRAPHY

1. Laue, K. and H. Stenger, Extrusion. Ohio: ASM, Metals Park, 1980
2. Shabaik, A., S. Kobayashi, and E.G. Thomsen, "Application of Potential Flow Theory to Plane-Strain Extrusion," Journal of Engineering for Industry, Vol. 89, pp. 503-505, August 1967.
3. Frisch, J. and E. G. Thomsen, "An Experimental Study of Metal Extrusions at Various Strain Rates," Trans. Am. Soc. Mech. Engrs., Vol. 76, pp. 599-601, May 1954
4. Yang, C.T. and J. Frisch, "Plastic Flow in a Lead Extrusion," Trans. Am. Soc. Mech. Engrs., Vol. 75, pp. 575-579, May 1953.
5. Matsuura, Y. and A Fujita; "Some Problems about Lead Extrusion," Report of the Casting Research Laboratory, Waseda University, No. 15, pp. 31-36, 1964.
6. Pearson, C.E. and R.N. Parkins, The Extrusion of Metals. New York: John Wiley, 1960.
7. Purchase, N.W. and S.J. Tupper, "Experiments with a Laboratory Extrusion Apparatus under Conditions of Plane Strain" Journal of the Mechanics and Physics of solids, Vol. 1, pp. 277-283, 1953.
8. Frisch, J. and E.G. Thomsen, "The Effect of Process Variables on Extrusion Pressures of Lead," Journal of Engineering for Industry, Vol. 80, pp. 207-215, August 1959.
9. Thomsen, E.G. and J. Frisch, "Experimental and Theoretical Pressures and Velocity Fields for Various Lead Extrusions" Trans. Am. Soc. Mech. Engrs., Vol. 80, pp. 117-123, Jan. 1958

10. Thomsen, E.G. and J. Frisch, "Stresses and Strains in Cold Extruding 2S-O Aluminium," Trans. Am. Soc. Mech. Engrs., Vol. 77, pp. 1343-1351, November 1955.
11. Avitzur, B., "Analysis of Central Bursting Defects in Extrusion and Wire Drawings," Journal of Engineering for Industry, Vol. 90, pp. 79-91, February 1968.
12. Avitzur, B., "Strain-Hardening and Strain-Rate Effects in Plastic Flow through Conical Converging Dies," Journal of Engineering for Industry, Vol. 89, pp. 556-562, August 1967.
13. Avitzur, B., "Analysis of Wire Drawing and Extrusion through Conical Dies of Large Cone Angle," Journal of Engineering for Industry, Vol. 86, pp. 305-315, November 1964.
14. Avitzur, B., "Analysis of Metal Extrusion," Journal of Engineering for Industry, Vol. 87, pp. 57-70, February 1965.
15. Avitzur, B., J. Fueyo, and J. Thompson, "Analysis of Plastic Flow through Inclined Planes in Plane Strain," Journal of Engineering for Industry, Vol. 89, pp. 361-375, May 1967.
16. Shabaik, A.H. and E.G. Thomsen, "A Theoretical Method for the Analysis of Metal-Working Problems," Journal of Engineering for Industry, Vol. 90, pp. 343-352, May 1968.
17. Iwata, K., K. Osakada, and S. Fujino, "Analysis of Hydrostatic Extrusion by the Finite Element Method," Journal of Engineering for Industry, Vol. 94, pp. 697-703, May 1972.

18. Medrano, L.E., C.P. Hinesley, P.P. Gillis, And H. Conrad
"Visioplasticity Analysis of 2024 Aluminium Alloy Extrusions,
"International Journal of Mechanical Sciences, Vol. 15,
pp. 955-965, 1973.
19. Sheppard, T., "Temperature and Speed Effects in Hot
Extrusion of Aluminium Alloys," Metals Technology, Vol.
8, pp. 130-141, April 1981.
20. Stater, R.A.C., Engineering Plasticity. London: The
Macmillan Press Ltd., 1977.
21. Bishop, J.F.W., "The Theory of Extrusion," Metallurgical
Reviews, Vol. 2, No. 8, pp. 361-390, 1957.
22. Backofen, W.A., Fundamentals of Deformation Processing.
New York: Syracuse University Press, 1964.
23. Sandin. A., "The Origin of the Extrusion Defect in
Copper and α/β Brass," Journal of the Institute of metals,
Vol. 61, pp. 439-444, 1961.
24. Unksov, E.P., An Engineering Theory of Plasticity.
London: The Macmillan Press Ltd., 1961.
25. Kennicott, W.L., "Carbide Tools for Cold Extrusion,"
Metals Engineering Quarterly, Vol. 73 , pp. 218-225, 1973
26. Braun, A., "Designing for Cold Extrusion," Metals
Progress, Vol. 75, pp.201-204, 1962.
27. Korytko, M.I., "Technical Aspects of Forward Cold Extrusion,"
Precision Metal, Vol. 78, pp. 31-32, February 1978
28. Metals Handbook, Properties and Selection of Metals. 2nd
ed., Ohio: ASM, Metals Park, 1961.

29. Altıntaş, S., "AlMgSi0.5 Ekstrüzyonu ve Mekanik Özelliklerine Etki Eden Parametreler " Fen Bilimleri Enstitüsü, Boğaziçi Üniversitesi, FBE/MM 84-01, Aralık 1984.
30. Makine Mühendisliği El Kitabı, Malzeme ve Yapım Yöntemleri, 2.Cilt, Ankara: TMMOB, Makine Mühendisleri Odası, 1976